increased in mock- and Wt-Ba/F3, but remained low in *JAK2V617F*-Ba/F3. Conversely, $p21^{WAF1}$ slightly decreased unexpectedly in IL-3-deprived mock- and Wt-Ba/F3, whereas it remained nearly the same in *JAK2V617F*-Ba/F3 (Fig. 1A). However, the proteasome inhibitor lactacystin induced the $p27^{Kip1}$ protein of *JAK2V617F*-Ba/F3 (Fig. 1B). In our model, cyclin D1 and D3, another cell cycle regulators, did not seem to play a major role in *JAK2V617F*-Ba/F3.

Inhibition of $p27^{Kip2}$ by JAK2V617F through SKP2 activation

Reportedly, $p27^{Kip1}$ was regulated by protein degradation rather than by transcriptional activation [16]. Recently, the relationship between $p27^{Kip1}$ and BCR/ABL has been reported using *BCR/ABL* stable transfectants [7]. Fig. 1A showed that Skp2 was decreased by IL-3 depletion in mock- and Wt-Ba/F3 but not in *JAK2V617F*-Ba/F3 cells. We also examined $p27^{Kip1}$ protein expression of *BCR/ABL*-, *STAT5 1*6* (constitutive active)- and *STAT3C* (constitutively active)-Ba/F3 cells with or without IL-3. Results showed that increase of $p27^{Kip1}$ protein induced with IL-3 deprivation was observed in wild type-*STAT* stable transfectants but not in constitutively active counterparts (Fig. 1C). Similarly, *BCR/ABL*-Ba/F3 showed high Skp2 protein in IL-3 depleted culture (Fig. 1D).

Skp2 mRNA level after IL-3 depletion

Fig. 2 illustrates semi-quantitative RT-PCR assay of $p27^{Kip1}$ and *Skp2* mRNAs in mock-, *JAK2V617F*-, *MIG*-mock- (as the control of *BCR/ABL* transfectant) and *BCR/ABL*-Ba/F3 cells. Semi-quantitative RT-PCR of $p27^{Kip1}$ mRNA showed that the $p27^{Kip1}$ message did not change significantly regardless of IL-3 presence. Therefore, the regulation of $p27^{Kip1}$ protein may not have taken place at the transcription level, although our preliminary promoter assay of $p27^{Kip1}$ revealed that the region between −348 and −2 bp was responsible for $p27^{Kip1}$ gene expression. On the contrary, it clearly shows that IL-3 depletion reduced *Skp2* mRNA in mock-cells, whereas *JAK2V617F*- and *BCR/ABL*-Ba/F3 did not show a similar decrease of mRNA, suggesting that maintaining *Skp2* mRNA level in *JAK2V617F*- and *BCR/ABL*-Ba/F3 cells is important for inhibiting the increase of the $p27^{Kip1}$ protein level after IL-3 depletion.

Determination of STAT site of Skp2 promoter

Next, we examined *Skp2* promoter analysis using a luciferase vector containing the 5′-promoter of *Skp2*. Fig. 3 shows the results of IL-3 depleted *JAK2V7617F*- and *BCR/ABL*-Ba/F3 cells. It suggests that a STAT motif located between −167 and −116 bp from the first exon (the second distal one in the inlet of Fig. 3A) was responsible for *JAK2V617F* as well as *BCR/ABL*.

EMSA and Chip assay of Skp2

Fig. 4 illustrates the results of EMSA. Among three bands observed, band *a* was produced with the wild type-oligo probe but not with the mutated-oligo in *JAK2V617F*-Ba/F3, and was erased with the cold competitor, suggesting its specificity (Fig. 4B and C). The intensity of band *c* is variable among experiments. Supershift assay using anti-STAT3 and anti-STAT5 antibody showed that anti-STAT5 antibody produced a supershifted band (Fig. 4D, asterisk). Anti-STAT3 antibody did not reduce band *a*. ChIP assay (Fig. 4E) suggests that STAT5 but not STAT3 was bound to the STAT site of the 5′-promoter, which is consistent with our EMSA.

Discussion

JAK2 is a member of the signal transducers located downstream of cellular receptors such as EPO receptor, IL-3 receptor, and GM-CSF receptor, and plays a critical role in the proliferation and differentiation of hematopoietic cells [17]. Recent studies revealed that a

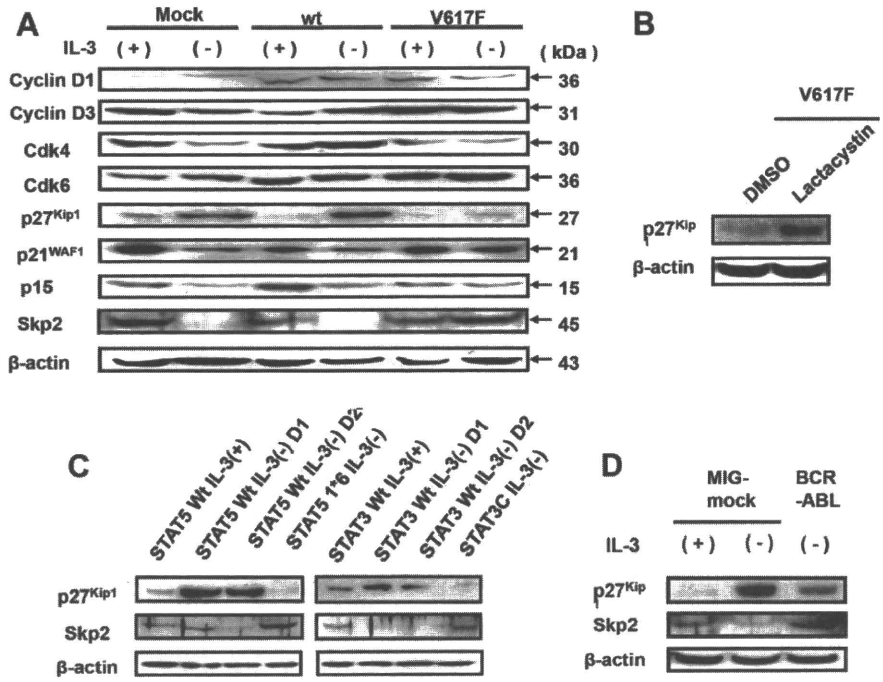

Fig. 1. Change of cell cycle regulators and related proteins in mock-, Wt- and *JAK2V617F*-Ba/F3 cells. (A) Protein levels of several cell cycle regulatory proteins including Cyclin D1, Cyclin D3, Cdk4, Cdk6, $p27^{kip1}$, $p21^{WAF1}$, p15 and SKP2 in mock-, Wt- and *JAK2V617F*-Ba/F3 were measured after 48 h with (+) or without (−) IL-3 addition. β-Actin was shown as the internal control. (B) The effect of lactacystin on P27 expression was examined using *JAK2V617F*-Ba/F3 cells. DMSO-treated cells were used as the vehicle control. (C) Stably overexpressed wild-type *STAT3*-, *STAT5*- and constitutive *STAT3* (*STAT3C*)-, and constitutive *STAT5* (*Stat5 1*6*)-Ba/F3 cells were examined for their p27 and Skp2 expression with or without IL-3 by Western blotting. (D) Using MIG-mock- and *BCR/ABL*-Ba/F3 cells, protein levels of p27 and Skp2 were analyzed by Western blotting.

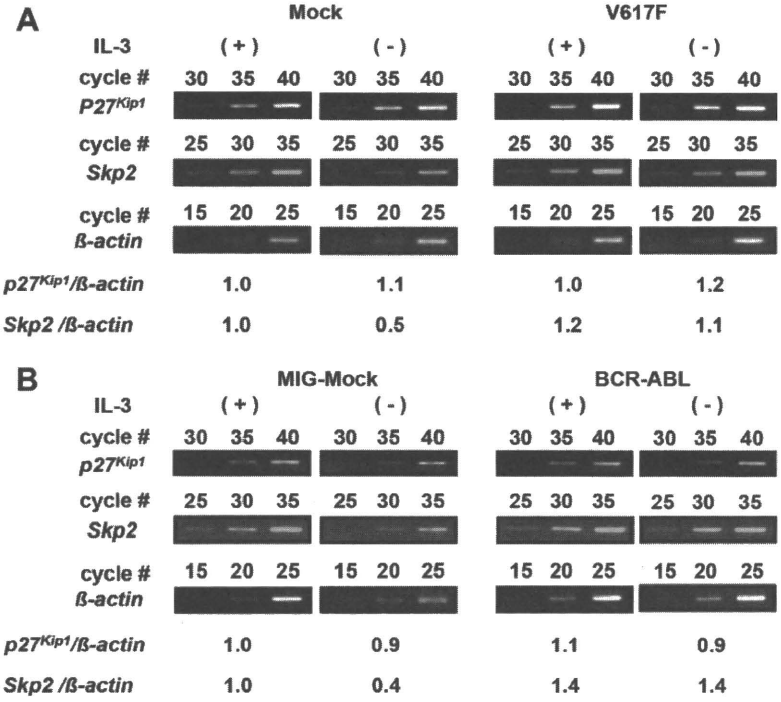

Fig. 2. *p27*^{Kip1} and *Skp2* mRNA expression of *JAK2V617F*-Ba/F3 and *BCR/ABL*-Ba/F3. *p27*^{Kip1} and *Skp2* mRNAs of mock-, *JAK2V617F*- and *BCR/ABL*-Ba/F3 were measured by the semi-quantitative RT-PCR method as described in Materials and methods. IL-3 (+) and IL-3 (−) denote cells cultured with or without Il-3 for 24 h. The relative expression level was calculated as the respective mRNA/β-actin mRNA. IL-3 treated culture was regarded as 1.0, respectively. A typical result was shown among several similar experiments.

high proportion of myeloproliferative disorder patients harbor a unique point mutation of *JAK2* [1,18]. It is also known that *JAK2V617F* mutation causes a gain of function of the JH2 domain, which inhibits the overactivation of the JH1 domain and controls its function [19]. This activated kinase might induce the change in the gene expression profile, which leads to the growth advantage of the MPD clone.

In the current study, we tried to elucidate the aberrant expression mechanism of the target protein of *JAK2V617F*. The p27^{Kip1} protein of *JAK2V617F*-Ba/F3 did not increase in the confluent state or cytokine depletion, whereas it increased in mock-Ba/F3, suggesting that *JAK2V617F* affects the cellular mechanism maintaining a normal cell growth character. However, increased p27^{Kip1} protein of *JAK2V617F*-Ba/F3 cells treated with a proteasome inhibitor,

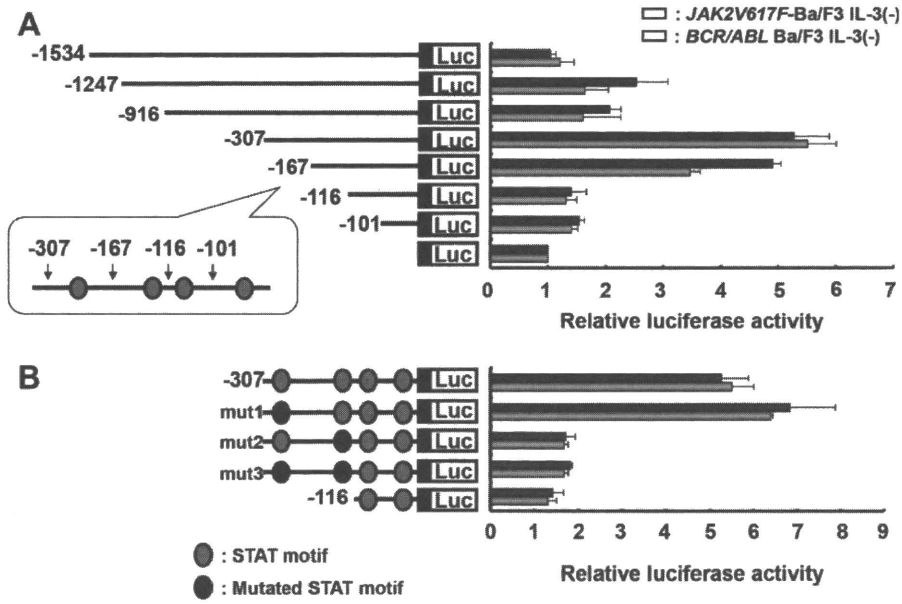

Fig. 3. Promoter analysis of *Skp2*. (A) Using *JAK2V617F*-Ba/F3 and *BCR/ABL*-Ba/F3 cells, the promoter activity of *Skp2* gene was analyzed by transfecting a pGL3 basic reporter containing various lengths of the 5′-promoter region as described in Materials and methods. Results were shown as the ratio of luciferase/β-gal. Data of pGL3 without insert was regarded as 1.0. Four STAT motifs located upstream of the first exon were illustrated on the left (solid gray circles). (B) The same experiments were carried out using mutated luciferase vectors. Solid grey and black circles denote wild and mutated STAT motif, respectively. The mean± was calculated from three independent experiments.

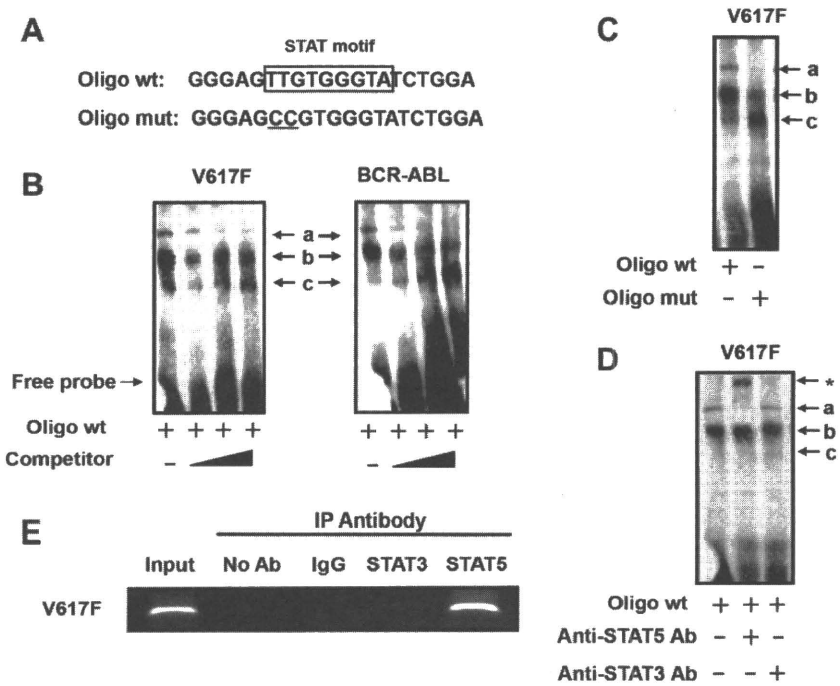

Fig. 4. EMSA and ChIP assay of *Skp2*. (A) Wild-type and mutated-oligoprobes used for EMSA of *Skp2* were shown as Oligo wt and Oligo mut. The STAT binding motif was boxed. Mutated bases are underlined. (B) EMSA was performed using *JAK2V617F*-Ba/F3 and *BCR/ABL*-Ba/F3 nuclear extracts, three bands (A–C) were observed. Cold competitor (5–20×) was added as indicated. (C) EMSA was performed using biotin-labeled wild or mutated-oligos shown in (A). (D) Anti-STAT3 and anti-STAT5 antibodies were used for the supershift assay according to Materials and methods. Shifted band was indicated by an asterisk. (E) ChIP assay was performed using anti-STAT3, anti-STAT5 antibody, normal mouse IgG and no antibody addition. Nuclear extract was prepared from *JAK2V617F*-Ba/F3 cells. A PCR primer set was described in Materials and methods.

lactacystin, suggests that $p27^{Kip1}$-related cell cycle regulation was not totally out of order in *JAK2V617F*-Ba/F3. On the contrary, $p21^{WAF1}$ of Ba/F3 cells might not be the major cell cycle regulator as suggested by others [20].

In colon carcinoma tumors and cell lines, Lin et al. reported the silencing of the JAK3/STAT3-induced increase in $p21^{WAF1}$ and $p27^{Kip1}$, suggesting that the JAK/STAT pathway inhibits these cell cycle regulators [21]. Although a STAT binding site is reported to be responsible for G-CSF-induced $p27^{Kip1}$ gene expression in 32D cells [22], our RT-PCR analysis suggests that aberrant $p27^{Kip1}$ gene expression was not the cause of the low $p27^{Kip1}$ protein level observed in *JAK2V617F*-Ba/F3. Our promoter analysis of $p27^{Kip1}$ could not detect any possible negative regulatory domain (data not shown).

Recently, Agarwal et al. [7] reported that *BCR/ABL* inhibits p27 expression through overexpression of SKP2, the F-box protein of the E3 ligase SCF^{SKP2}. The inverse relationship between Skp2 and p27 and oncogenic role of SKkp2 in primary cancer have been reported [23,24]. However, the relevant mechanism of Skp2 overexpresion by JAK2V617F/STAT pathway has not been elucidated. We determined for the first time the target STAT site of the 5′-promoter of *Skp2* responsible for *JAK2V617F* and *BCR/ABL* mutations. Although both *JAK2V617F* and *BCR/ABL* activate STAT5 and STAT3, our current analysis showed that STAT5 was more potent in binding to STAT motifs of the 5′-promoter of *Skp2* than STAT3 (Fig. 4D and E). Because overexpression of the constitutively active STAT3 could mimic *JAK2V617F*, the negative results of supershift and ChIP shown in Fig. 4 might be due to the anti-STAT3 antibody we used.

Furthermore, we also found high $Bcl\text{-}x_L$ mRNA in *JAK2V617F*-Ba/F3 as well as *BCR/ABL*-Ba/F3 cells and identified the responsible STAT motif in the 5′-promoter of $Bcl\text{-}x_L$ (data not shown). This may also contribute the pathogenesis of *JAK2V617F* mutation and of *BCR/ABL* translocation. Taken together, in the current study, the defective $p27^{Kip1}$ expression in response to cytokine depletion was characterized in *JAK2V617F*-Ba/F3 as well as *BCR/ABL*-Ba/F3. It is demonstrated a cell cycle regulator of $p27^{Kip1}$, and an E3 ligase subunit of Skp2, are finely controlled in Ba/F3 cells, but not in the presence of *JAK2V617F*. Future control of this particular pathway could help MPD as well as CML therapies.

Appendix A. Supplementary data

Supplementary data associated with this article can be found, in the online version, at doi:10.1016/j.bbrc.2009.04.015.

References

[1] R. Kralovics, F. Passamonti, A.S. Buser, S.S. Teo, R. Tiedt, J.R. Passweg, A. Tichelli, M. Cazzola, R.C. Skoda, A gain-of-function mutation of JAK2 in myeloproliferative disorders, N. Engl. J. Med. 352 (2005) 1779–1790.
[2] L.M. Scott, M.A. Scott, P.J. Campbell, A.R. Green, Progenitors homozygous for the V617F mutation occur in most patients with polycythemia vera, but not essential thrombocythemia, Blood 108 (2006) 2435–2437.
[3] J. Kota, N. Caceres, S.N. Constantinescu, Aberrant signal transduction pathways in myeloproliferative neoplasms, Leukemia 22 (2008) 1828–1840.
[4] P. Saharinen, O. Silvennoinen, The pseudokinase domain is required for suppression of basal activity of Jak2 and Jak3 tyrosine kinases and for cytokine-inducible activation of signal transduction, J. Biol. Chem. 277 (2002) 47954–47963.
[5] M. Pless, K. Norga, M. Carroll, M.H. Heim, A.D. D'Andrea, B. Mathey-Prevot, Receptors that induce erythroid differentiation of Ba/F3 cells: structural requirements and effect on STAT5 binding, Blood 89 (1997) 3175–3185.
[6] I.M. Chu, L. Hengst, J.M. Slingerland, The Cdk inhibitor p27 in human cancer: prognostic potential and relevance to anticancer therapy, Nat. Rev. Cancer 8 (2008) 253–267.
[7] A. Agarwal, T.G. Bumm, A.S. Corbin, T. O'Hare, M. Loriaux, J. VanDyke, S.G. Willis, J. Deininger, K.I. Nakayama, B.J. Druker, M.W. Deininger, Absence of SKP2 expression attenuates BCR-ABL-induced myeloproliferative disease, Blood 112 (2008) 1960–1970.
[8] E.J. Andreu, E. Lledo, E. Poch, C. Ivorra, M.P. Albero, J.A. Martinez-Climent, C. Montiel-Duarte, J. Rifon, J. Perez-Calvo, C. Arbona, F. Prosper, I. Perez-Roger, BCR–ABL induces the expression of Skp2 through the PI3K pathway to promote p27Kip1 degradation and proliferation of chronic myelogenous leukemia cells, Cancer Res. 65 (2005) 3264–3272.

[9] K. Shide, K. Shimoda, K. Kamezaki, H. Kakumitsu, T. Kumano, A. Numata, F. Ishikawa, K. Takenaka, K. Yamamoto, T. Matsuda, M. Harada, Tyk2 mutation homologous to V617F Jak2 is not found in essential thrombocythaemia, although it induces constitutive signaling and growth factor independence, Leuk. Res. 31 (2007) 1077–1084.
[10] T. Nosaka, T. Kawashima, K. Misawa, K. Ikuta, A.L. Mui, T. Kitamura, STAT5 as a molecular regulator of proliferation, differentiation and apoptosis in hematopoietic cells, EMBO J. 18 (1999) 4754–4765.
[11] K. Nakajima, Y. Yamanaka, K. Nakae, H. Kojima, M. Ichiba, N. Kiuchi, T. Kitaoka, T. Fukada, M. Hibi, T. Hirano, A central role for Stat3 in IL-6-induced regulation of growth and differentiation in M1 leukemia cells, EMBO J. 15 (1996) 3651–3658.
[12] Y. Kato, A. Iwama, Y. Tadokoro, K. Shimoda, M. Minoguchi, S. Akira, M. Tanaka, A. Miyajima, T. Kitamura, H. Nakauchi, Selective activation of STAT5 unveils its role in stem cell self-renewal in normal and leukemic hematopoiesis, J. Exp. Med. 202 (2005) 169–179.
[13] Y. Chalandon, X. Jiang, O. Christ, S. Loutet, E. Thanopoulou, A. Eaves, C. Eaves, BCR–ABL-transduced human cord blood cells produce abnormal populations in immunodeficient mice, Leukemia 19 (2005) 442–448.
[14] S. Sobue, K. Hagiwara, Y. Banno, K. Tamiya-Koizumi, M. Suzuki, A. Takagi, T. Kojima, H. Asano, Y. Nozawa, T. Murate, Transcription factor specificity protein 1 (Sp1) is the main regulator of nerve growth factor-induced sphingosine kinase 1 gene expression of the rat pheochromocytoma cell line, PC12, J. Neurochem. 95 (2005) 940–949.
[15] S. Sobue, M. Murakami, Y. Banno, H. Ito, A. Kimura, S. Gao, A. Furuhata, A. Takagi, T. Kojima, M. Suzuki, Y. Nozawa, T. Murate, V-Src oncogene product increases sphingosine kinase 1 expression through mRNA stabilization: alteration of AU-rich element-binding proteins, Oncogene 27 (2008) 6023–6033.
[16] J. Hulit, R.J. Lee, Z. Li, C. Wang, S. Katiyar, J. Yang, A.A. Quong, K. Wu, C. Albanese, R. Russell, D. Di Vizio, A. Koff, S. Thummala, H. Zhang, J. Harrell, H. Sun, W.J. Muller, G. Inghirami, M.P. Lisanti, R.G. Pestell, P27Kip1 repression of ErbB2-induced mammary tumor growth in transgenic mice involves Skp2 and Wnt/beta-catenin signaling, Cancer Res. 66 (2006) 8529–8541.
[17] S.J. Baker, S.G. Rane, E.P. Reddy, Hematopoietic cytokine receptor signaling, Oncogene 26 (2007) 6724–6737.
[18] C. James, V. Ugo, J.P. Le Couedic, J. Staerk, F. Delhommeau, C. Lacout, L. Garcon, H. Raslova, R. Berger, A. Bennaceur-Griscelli, J.L. Villeval, S.N. Constantinescu, N. Casadevall, W. Vainchenker, A unique clonal JAK2 mutation leading to constitutive signalling causes polycythaemia vera, Nature 434 (2005) 1144–1148.
[19] P. Saharinen, M. Vihinen, O. Silvennoinen, Autoinhibition of Jak2 tyrosine kinase is dependent on specific regions in its pseudokinase domain, Mol. Biol. Cell 14 (2003) 1448–1459.
[20] H. Prietzsch, J. Brock, H.D. Kleine, S. Liebe, R. Jaster, Interferon-alpha inhibits cell cycle progression by Ba/F3 cells through the antagonisation of interleukin-3 effects on key regulators of G(1)/S transition, Cell. Signal. 14 (2002) 751–759.
[21] Q. Lin, R. Lai, L.R. Chirieac, C. Li, V.A. Thomazy, I. Grammatikakis, G.Z. Rassidakis, W. Zhang, Y. Fujio, K. Kunisada, S.R. Hamilton, H.M. Amin, Constitutive activation of JAK3/STAT3 in colon carcinoma tumors and cell lines: inhibition of JAK3/STAT3 signaling induces apoptosis and cell cycle arrest of colon carcinoma cells, Am. J. Pathol. 167 (2005) 969–980.
[22] J.P. de Koning, A.A. Soede-Bobok, A.C. Ward, A.M. Schelen, C. Antonissen, D. van Leeuwen, B. Lowenberg, I.P. Touw, STAT3-mediated differentiation and survival and of myeloid cells in response to granulocyte colony-stimulating factor: role for the cyclin-dependent kinase inhibitor p27(Kip1), Oncogene 19 (2000) 3290–3298.
[23] S. Davidovich, O. Ben-Izhak, M. Shapira, B. Futerman, D.D. Hershko, Over-expression of Skp2 is associated with resistance to preoperative doxorubicin-based chemotherapy in primary breast cancer, Breast Cancer Res. 10 (2008) R63.
[24] M. Rosner, M. Hanneder, N. Siegel, A. Valli, C. Fuchs, M. Hengstschlager, Skp2 inversely correlates with p27 and tuberin in transformed cells. Amino Acids (2008).

Ann Hematol (2010) 89:1255–1263
DOI 10.1007/s00277-010-1020-3

ORIGINAL ARTICLE

Autoantibodies specific to hnRNP K: a new diagnostic marker for immune pathophysiology in aplastic anemia

Zhirong Qi · Hiroyuki Takamatsu · J. Luis Espinoza · Xuzhang Lu · Naomi Sugimori · Hirohito Yamazaki · Katsuya Okawa · Shinji Nakao

Received: 2 February 2010 / Accepted: 16 June 2010 / Published online: 10 July 2010

Abstract To identify a new diagnostic marker for the immune pathophysiology of aplastic anemia (AA), we screened sera of immune-mediated AA patients for the presence of antibodies (Abs) specific to proteins derived from a leukemia cell line UT-7 using two-dimensional electrophoresis followed by immunoblotting. The target proteins were identified by peptide mass fingerprinting. Heterogeneous nuclear ribonucleoprotein (hnRNP) K was identified as a novel autoantigen. An enzyme-linked immunosorbent assay revealed high titers of anti-hnRNP K Abs in 85 (31%) of 273 patients with AA. Sixty-four patients received antithymocyte globulin and cyclosporine after undergoing screening for anti-hnRNP K Ab, anti-DRS-1 Ab, anti-moesin Ab, and paroxysmal nocturnal hemoglobinuria (PNH)-type cells. Twenty (87%) of 23 patients with the presence of anti-hnRNP K Abs responded to the immunosuppressive therapy (IST), while 19 (46%) of 41 patients without the presence of anti-hnRNP K Abs responded. A multivariate analysis showed only PNH-type cells and anti-hnRNP K Abs to be significant factors for the prediction of a good response to IST. The detection of anti-hnRNP K Abs as well as PNH-type cells may therefore be useful for diagnosing the immune pathophysiology of AA.

Keywords Aplastic anemia · hnRNP K · Autoantibody · Bone marrow failure

Z. Qi · H. Takamatsu · J. L. Espinoza · X. Lu · N. Sugimori · H. Yamazaki · S. Nakao (✉)
Cellular Transplantation Biology, Kanazawa University Graduate School of Medical Science,
13-1 Takaramachi,
Kanazawa 920-8641, Japan
e-mail: snakao@med3.m.kanazawa-u.ac.jp

Z. Qi
West China Medical Center, Sichuan University,
Chengdu, China

K. Okawa
Biomolecular Characterization Unit, Frontier Technology Center,
Kyoto University Graduate School of Medicine,
Kyoto, Japan

Introduction

A large amount of laboratory and clinical data including a good response to immunosuppressive therapy (IST) suggest that the immune system attack against hematopoietic stem cells plays an essential role in the pathophysiology of aplastic anemia (AA). More than 70% of all patients with AA respond to IST with antithymocyte globulin (ATG) and cyclosporine (CsA) [1, 2]. However, IST may be detrimental to patients with non-immune-mediated AA because it potentially increases the risk of opportunistic infections and delays treatment with allogeneic stem cell transplantation. Several markers predicting good response to IST in patients with AA have been proposed. These include an increased ratio of activated T cells [3], increased interferon-γ expression in bone marrow (BM) and peripheral blood T cells [4, 5], increased expression of heat shock protein 72 [6], the presence of HLA-DRB1*1501, and small population of paroxysmal nocturnal hemoglobinuria (PNH)-type cells [7, 8]. Recent studies have demonstrated the presence of PNH-type cells to be the most reliable predictor of good response to IST [9]. However, the method for detecting small populations of PNH-type cells has not yet been generalized, possibly due to inter-lab differences in the sensitivity and the specificity of flow cytometry. PNH-type cells cannot be utilized to diagnose immune pathophysiology when fresh blood containing a sufficient number of granulocytes from patients is unavailable. Furthermore,

approximately 48% of AA patients not bearing small populations of PNH-type cells (PNH^- patients) respond to ATG and CsA therapy [8]. More reliable and universal assays that supplement the role of PNH-type cell detection are therefore required to predict a good response to IST in patients with AA.

Autoimmune diseases such as multiple sclerosis (MS) and insulin-dependent diabetes mellitus (IDDM) are characterized by the presence of autoantibodies (auto-Abs) specific to antigens derived from target organs, such as myelin basic protein in MS and glutamate decarboxylase in IDDM. These autoantibodies are detectable in the patients' sera, and the Abs serve as a marker of the immune pathophysiology of these diseases [10, 11]. Two auto-Abs specific to diazepam-binding inhibitor-related protein-1 (DRS-1) and moesin were recently identified in the sera of patients with AA. These Abs were detectable in 38% and 37% of AA patients bearing increased PNH-type cells (PNH^+ patients), but the prevalence of the Abs in PNH^- patients with AA was only 6% and 21%, respectively [12, 13]. Therefore, these Abs do not help in the diagnosis of the immune pathophysiology in PNH^- patients with AA. The identification of novel auto-Abs is therefore needed to improve the accuracy of predicting good response to IST.

This study screened sera from patients with PNH^+ AA for the presence of Abs recognizing antigens derived from a megakaryocytic leukemia cell line UT-7 using two-dimensional electrophoresis (2-DE) followed by immunoblotting and peptide mass fingerprinting.

Materials and methods

Sera and cell lines

Sera were obtained from 273 Japanese patients with AA at the time of the diagnosis. Table 1 shows characteristics of patients with AA. AA was diagnosed at Kanazawa University hospital and other hospitals taking part in the bone marrow failure (BMF) study group led by the Ministry of Health, Labor, and Welfare of Japan from December 2007 to March 2009. Sera were also obtained from 33 Japanese patients with rheumatoid arthritis (RA). Sera from 96 healthy individuals were used as controls. Samples were cryopreserved at −80°C until use. UT-7 was kindly provided by Dr N. Komatsu of Jichi Medical School. OUN-1, a cell line derived from chronic myelogenous leukemia, was kindly provided by Dr M. Yasukawa of the Ehime University. K562 and HL-60 cell lines were purchased from the Health Science Research Resource Bank (Osaka, Japan). All patients and healthy individuals provided their informed consent in accordance with the Declaration of Helsinki before sampling. This study was approved by the human research ethical committee of Kanazawa University Graduate School of Medical Science.

Table 1 Patient characteristics

Characteristics	Number	Range
Total (*n*)	273	NA
Age at diagnosis (year)	52.7	14–91
Gender (male/female)	141/132	NA
Severity (severe/moderate)	118/155	NA
Neutrophil count ($\times 10^9$/L)	830	0–2,325
Platelet count ($\times 10^9$/L)	22	2–126
Reticulocyte count ($\times 10^9$/L)	29	2–114

NA not applicable

Detection of PNH-type cells

Peripheral blood was subjected to high-sensitivity two-color flow cytometry to detect small populations of glycosylphosphatidylinositol-anchored membrane protein-deficient cells in granulocytes and erythrocytes, as described previously [8]. The presence of ≥0.003% $CD55^-CD59^-CD11b^+$ granulocytes and ≥0.005% $CD55^-CD59^-$glycophorin-A^+ erythrocytes was defined as an abnormal increase based on the results of 183 healthy individuals [9].

2-DE and western blotting

2-DE was performed as described previously with some modifications [14]. A total of 10^6 UT-7 cells were solubilized with sample preparation solution containing 7 M urea, 2 M thiourea, 4% CHAPS, 2% immobilized pH gradients (IPG) buffer pH 3–10, and 40 mM dithiothreitol (DTT; GE Healthcare, Tokyo, Japan), and the sample was diluted to 125 μl with thiourea rehydration buffer containing 7 M urea, 2 M thiourea, 2% IPG-buffer pH 3–10, 0.002% bromophenol blue, and 2.8 mg/ml DTT. Before loading into IPG-strips, the diluted sample was cleared by centrifugation (13,000 rpm for 20 min), applied to 7-cm non-linear Immobiline DryStrip of pH 3–10 (GE Healthcare) and incubated for 12 h at room temperature; then the IPG strip was subjected to first-dimensional isoelectric focusing electrophoresis (IFE) using the flatbed multiphor II electrophoresis system (GE Healthcare). The IPG strip after IFE was equilibrated twice at room temperature for 10 min with 10 ml of SDS equilibration buffer solution (6 M urea, 75 mM Tris–HCl pH 8.8, 29.3% glycerol, 2% SDS, 0.002% bromophenol blue, and 100 mg DTT or 250 mg iodoacetamide) and subjected to second dimensional SDS-PAGE. Separated proteins were transferred onto a polyvinylidene fluoride (PVDF) membrane (Millipore

Corporation, Bedford, USA) for 1.5 h at a constant current of 190 mA using a Mini Trans-Blot system (Bio-Rad, Hercules, CA) or visualized by Coomassie Brilliant Blue (CBB) staining. The blotted PVDF membranes were incubated in the presence of Tris-buffered saline (TBS) with 1% bovine serum albumin (BSA) containing serum diluted 1:200 from the patients, serum diluted 1:200 from healthy individuals or 1:2,000 diluted mouse anti-human heterogeneous nuclear ribonucleoprotein (hnRNP) K/J monoclonal Ab (mAb, clone 3C2, Sigma, USA), and then were reacted with appropriate alkaline phosphatase-labeled secondary Abs and the immunoblots were detected using a BCIP/NBT membrane alkaline phosphatase substrate system (KPL, Gaithersburg, MD, USA).

Isolation of $CD34^+$ cell

$CD34^+$ cells were isolated from the BM of healthy volunteers using a CD34 progenitor cell isolation kit (Miltenyi Biotec, Bergisch Gladbach, Germany) according to the manufacturer's instructions.

Protein identification

The proteins recognized by serum Abs were identified as previously describe [15, 16]. Briefly, after SDS-PAGE, proteins were visualized by CBB staining, and the pieces of the gel corresponding to western blotting-positive spots were excised, followed by in-gel digestions with trypsin. Molecular mass analyses of tryptic peptides were performed by matrix-assisted laser desorption/ionization time of flight mass spectrometry (MALDI-TOF MS) using an ultraflex TOF/TOF system.

Construction of the recombinant plasmid and purification of bacterially expressed protein

Full-length hnRNP K cDNA kindly provided by H. Sorimachi (Tokyo Metropolitan Organization for Medical Research) was subcloned into the pGEX-6p-1 vector (GE Healthcare) for the expression of glutathione-*S*-transferase (GST) fusion protein. Synthesized proteins were purified by glutathione sepharose 4B (GE Healthcare) according to the manufacturer's instructions. Native hnRNP K proteins were released from GST-hnRNP K fusion proteins using PreScission protease (GE Healthcare). The recombinant protein was confirmed by CBB staining and western blotting with anti-hnRNP K/J mAb.

Immunoprecipitation

Immunoprecipitation detection of anti-hnRNP K Abs using sera from patients with AA was performed according to the instructions of the Seize X Protein G Immunoprecipitation Kit (Pierce, Illinois, USA). Briefly, 10 μl of serum samples were incubated for 2 h at 4°C with 400 μl protein G-agarose beads (Pierce), and then the beads were washed three times with binding/wash buffer with centrifugation (10,000×*g* for 3 min). The beads were incubated in 200 μl of binding/wash buffer containing 1 μg of purified native hnRNP K protein for overnight at 4°C; then the beads were pelleted by centrifugation (10,000×*g* for 3 min). Thereafter, they were washed five times before the proteins were eluted from the beads with 50 μl of elution buffer for SDS-PAGE and western blotting with anti-hnRNP K/J mAb.

Determination of hnRNP K expression by hematopoietic cells

Lysates of myeloid leukemia cell lines, $CD34^+$, and peripheral blood mononuclear cells (PBMCs) from healthy individuals were obtained by suspending cell pellets in 100 μl of phosphate-buffered saline (PBS) containing protease inhibitor cocktail (Sigma Aldrich), sonicated on ice for 20 s using a B-12 Branson sonifier (Danbury, CT, USA). The cell lysates were then denatured in boiling SDS sample buffer. Equal amounts of proteins were separated by SDS-PAGE and transferred onto PVDF membrane. The membrane was incubated in 1% BSA–TBS containing 1:2,000 diluted anti-hnRNP K/J mAb or 1:5,000 diluted mouse anti-human α-tubulin mAb (clone B-5-1-2, Sigma, USA), respectively.

Enzyme-linked immunosorbent assay

Fifty microliters of coating buffer (50 mM carbonate/bicarbonate buffer, pH 9.6) containing 1 μg/ml recombinant native hnRNP K protein, recombinant native DRS-1 protein, or recombinant native moesin protein was added to each well of a 96-well Nunc-Immuno plate (Nalge-Nunc International, Roskilde, Denmark) and kept overnight at 4°C. The plates were washed and incubated with PBS containing 10% fetal bovine serum for 2 h at 37°C to block nonspecific binding. The sera from patients were added to a final dilution of 1:200 at room temperature for 2 h. After washing, the plates were incubated with 100 μl of peroxidase-conjugated goat anti-human IgG Ab (1:100,000; Jackson ImmunoResearch) at room temperature for 1 h. Finally, plates were washed and incubated with 3,3,5,5-tetramethylbenzidine substrate (Pierce, Rockford, IL) at room temperature for 30 min, and the optic density (OD) absorbance at 450 nm was read using a SLTEAR 340 ATELISA reader (SLT-Labinstruments, Grödig, Austria). A positive reaction (Ab^+) was defined as an absorbance value exceeding the mean+2 standard deviation (SD) of the OD absorbance values from the sera of the 96 healthy individuals.

Immunosuppressive therapy

Sixty-four patients with AA were treated with ATG (Lymphoglobuline, Aventis Behring, King of Prussia, PA) 15 mg/kg/day, 5 days, plus CsA (Novartis, Basel, Switzerland) 6 mg/kg/day within 1 year of diagnosis between December 2007 and March 2009. The dose of CsA was adjusted to maintain trough levels between 150 and 250 ng/ml, and the appropriate dose was administered for at least 6 months. Granulocyte colony-stimulating factor (G-CSF; filgrastim, 300 μg/m^2 or lenograstim, 5 μg/kg) was administered to some patients. The response to IST was assessed at 6 months after the IST according to the criteria proposed by Camitta [17].

Statistics

Differences in the prevalence of hnRNP K Abs among different groups were examined using a one-way analysis of variance. Correlations of anti-hnRNP K Ab titers with anti-moesin Ab titers or anti-DRS-1 Ab titers in individual patients were examined using student *t* test. The prevalence of anti-hnRNP K Abs between untransfused and transfused patients and the response rate to IST between Ab$^+$ and Ab$^-$ patients were examined using the Fisher's exact test. Logistic procedures and Fisher's exact test were used to analyze the associations between the response to IST and the prevalence of increased PNH-type cells, gender, age, severity, or three different Abs.

Results

Detection of novel auto-Abs in AA patients' sera

To detect auto-Abs specific to proteins derived from UT-7 cells, cell lysates were separated by 2-DE and subjected to western blotting using sera obtained from two PNH$^+$ untransfused patients with AA at the time of diagnosis. The sera from two patients revealed the same spot with a size of 65 kDa (Fig. 1a—ii) which was not seen on the membrane incubated with healthy individual sera (Fig. 1a—iii). The approximate isoelectric point was between 5 and 6.

Identification of the 65-kDa protein

The stained spot corresponding to the one showing positive reaction in the western blotting (Fig. 1a–i) was excised from the CBB stained gel. The proteins were eluted from the excised gel after in-gel enzyme digestion and were subjected to MALDI-TOF MS. The protein was identified as hnRNP K of which isoelectric point is 5.46. Anti-hnRNP K/J mAb revealed the same spot identified by the incubation with the patient sera (Fig. 1a—iv). Specific binding of the patients' anti-hnRNP K Abs to hnRNP K was confirmed by an immunoprecipitation analysis (Fig. 1b).

Expression of hnRNP K by hematopoietic cells

The level of expression of hnRNP K was greater in several myeloid leukemia cell lines such as HL-60, OUN-1, UT-7, and K562 than in PBMCs from healthy individuals, but there was no difference in the hnRNP K expression level between CD34$^+$ cells and PBMCs from healthy individuals (Fig. 2).

Prevalence of anti-hnRNP K Abs in patients with AA and RA

The titers of Ab specific to hnRNP K in the sera of 273 AA and 33 RA patients were determined using enzyme-linked immunosorbent assay (ELISA) with the recombinant human native hnRNP K proteins (Fig. 3a). The titers of Ab specific to hnRNP K in the sera of 273 AA and 33 RA patients were determined using ELISA with the recombinant human native hnRNP K proteins (Fig. 3a). High titers of anti-hnRNP K Abs (≥ the mean±2SD of the titers of healthy individuals, anti-hnRNP K Ab$^\pm$) were detected in 85 (31%) of the AA patients and in eight (24%) of the RA patients. There was no significant difference in the prevalence of anti-hnRNP K Abs between AA and RA patients ($P \geq 0.05$). There was no difference in the prevalence of anti-hnRNP K Abs between untransfused (27%) and transfused (33%) AA patients ($P = 0.33$). Small populations of PNH-type cells were detectable in 155 (56%) of the AA patients, and the prevalence of anti-hnRNP K Abs in PNH$^+$ and PNH$^-$ AA patients was 36% and 25%, respectively.

Correlation of anti-hnRNP K Abs with other auto-Abs

Anti-hnRNP K Ab with anti-DRS-1 Ab or anti-moesin Ab titers were measured from the same patients' sera to determine the relationship between these Abs. The anti-DRS-1 Abs and anti-moesin Abs were detectable in 29% and 28% of the 273 patients with AA, respectively. The titers of anti-hnRNP K Abs positively correlated with the presence of anti-DRS-1 Abs ($r = 0.5838$) and anti-moesin Abs ($r = 0.7239$; $P < 0.0001$; Fig. 3b).

Correlation of anti-hnRNP K Abs with response to IST

Sixty-four patients with AA of the 273 patients received ATG plus CsA therapy after the screening of three different

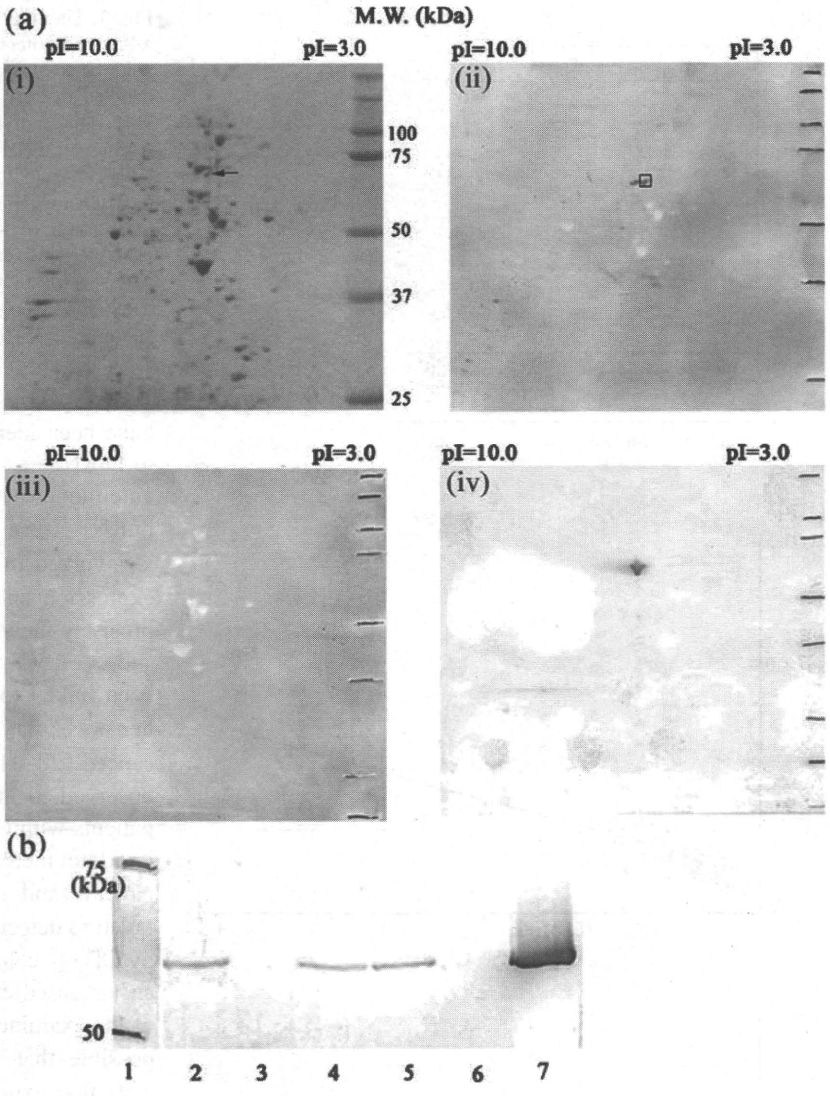

Fig. 1 Identification of the proteins derived from UT-7 cells recognized by serum Abs. **a** hnRNP K auto-Ab in serum from patient with AA. *i* UT-7 cell lysates were separated by 2-DE and visualized by CBB staining. The protein spot indicated by the *arrow* was identified as hnRNP K by mass spectrometry. *ii* UT-7 cell lysates were separated by 2-DE, transferred onto PVDF membrane, and then incubated with diluted AA patient serum (1:200). *iii* PVDF membrane was incubated with diluted healthy individual serum (1:200). *iv* PVDF membrane was incubated with diluted anti-hnRNP K/J mAb (1:2,000). **b** Immunoprecipitation detection of anti-hnRNP K Ab in the sera of patients with BMF. An equal amount of purified native hnRNP K proteins was incubated in the serum from AA patients (*lanes 2*, *4*, and *5*) and healthy individuals' sera (*lanes 3* and *6*). Anti-hnRNP K/J mAb at a 1:2,000 dilution was used as a positive control (*lane 7*)

Abs and PNH-type cells. Twenty (87%) of 23 patients with anti-hnRNP K Ab^+ responded to the IST, while 19 (46%) of 41 patients with anti-hnRNP K Ab^- responded (P=0.0015, Fig. 4a). When anti-hnRNP K Ab^+ patients were divided into two groups according to the Ab titers, there was no difference in the response rate to IST between very high titer (≥0.4, 93%) and moderately high titer (<0.4, 87%) groups (P=1.00). The response rate to IST in patients with at least one Ab^+ of three auto-Abs including anti-hnRNP K Ab, anti-DRS-1 Ab, and anti-moesin Ab was 81%, while the response rate in patients not showing Ab^+ in any of the three auto-Abs was 42% (P=0.0022; Fig. 4b). In 32 patients not displaying PNH-type cells, the response rate to IST with anti-hnRNP K Ab^+ was 86%, while only 32% patients with anti-hnRNP K Ab^- responded (P=0.0265; Fig. 4c). Multivariate analysis showed the presence of anti-hnRNP K Abs and PNH-type cells to be significant factors in the prediction of good response to IST (Table 2). Anti-hnRNP K Ab titers could be serially determined for 13 patients before and 6–7 months after IST. Four of the 13 patients showed high anti-hnRNP K Ab titers before IST. The Abs titers did not decrease either in three patients (pre-IST/post-IST: 0.3625/0.3635, 0.513/1.2455, 0.2875/0.2932) responding to IST or in one patient refractory to IST (0.413/0.318).

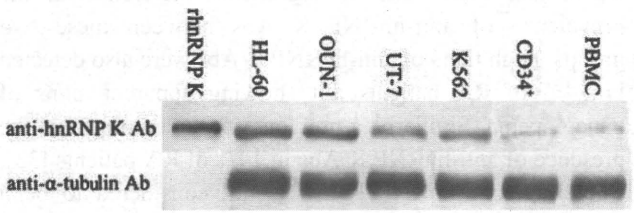

Fig. 2 Expression of hnRNP K by immature hematopoietic cells and PBMCs. An equal amount (20 μg) of cell extracts or recombinant hnRNP K protein was separated by 8% SDS-PAGE, transferred to PVDF membrane, and reacted with anti-hnRNP K/J mAb at a 1:2,000 dilution or anti-α-tubulin mAb at a 1:5,000 dilution

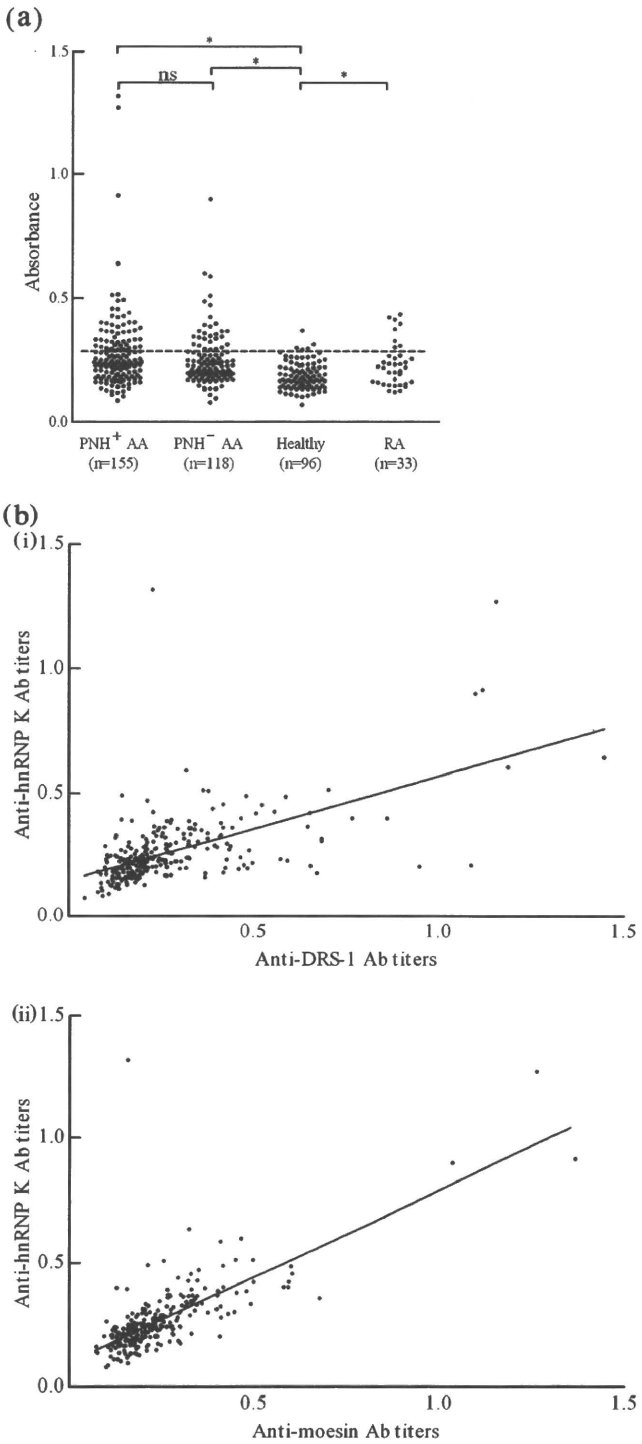

Fig. 3 Titration of anti-hnRNP K Abs in patients' sera using ELISA. **a** Antibody titers against purified hnRNP K proteins in the sera were determined using diluted sera at a 1:200 dilution. The *dotted line* denoted a cutoff value defined as the mean+2SD of the absorbance in 96 healthy individuals. *Asterisks* indicate a prevalence of hnRNP K Ab titers in PNH^+ AA, PNH^- AA, and RA patients' sera significantly higher than that of hnRNP K Ab titers in healthy individuals (*$P<0.05$; *ns* no significant meaning). **b** The correlation between the titers of anti-hnRNP K Ab and either anti-DRS-1 Ab or anti-moesin Ab from the same sera obtained from AA patients was examined. Titers of Abs specific to native hnRNP K, DRS-1, and moesin protein were determined using diluted sera at a 1:200 dilution, and correlations of anti-hnRNP K Ab titers with each of other two Ab titers (*i* and *ii*) were calculated ($P<0.0001$)

Discussion

The present study identified anti-hnRNP K Abs as a novel auto-Ab in the serum of patients with immune-mediated AA. hnRNPs are among the most abundant proteins in the eukaryotic cell nucleus and play a direct role in several aspects of RNA activity including splicing, export of the mature RNAs, and translation. Approximately 30 hnRNPs have been identified [18]. More and more evidence points to hnRNPs as important intracellular target antigens of the autoimmune response in autoimmune diseases [19–25]. hnRNP K is a conserved RNA/DNA-binding protein which is involved in the multiple steps that comprise both gene expression and signal transduction [26, 27]. It is unclear precisely how the anti-hnRNP K Abs were raised in a subset of AA patients. The overexpression of hnRNP K has been linked to a range of cancers including breast cancer, hepatocellular carcinoma, esophageal cancer, and colorectal cancer [28–31]. The hnRNP K protein expression was observed to increase in the $CD34^+$ bone marrow cells of patients with CML in the accelerated and blastic phase, but it did not increase in the $CD34^+$ cells of chronic phase CML patients and of healthy donors [32]. The present study failed to detect an increased expression of hnRNP K protein by $CD34^+$ cells from healthy individuals as well. However, an increased expression of hnRNP K was detectable in all of the examined myeloid leukemia cell lines. It is therefore possible that the destruction of immature hematopoietic cells that express high levels of hnRNP K may induce a specific immune response to hnRNP K in patients with immune-mediated AA.

The ELISA detected significantly higher titers of anti-hnRNP K Abs in comparison to healthy controls in 56 (36%) of 155 patients with immune-mediated AA displaying increased PNH-type cells and in 29 (25%) of 118 patients without increased PNH-type cells in the current study, and there was no significant difference in the prevalence of anti-hnRNP K Abs between these two groups. High titers of anti-hnRNP K Abs were also detected in 24% of RA patients not showing apparent signs of pancytopenia. Similarly, a previous study demonstrated the presence of anti-hnRNP K Abs in 14% of RA patients [33]. Therefore, anti-hnRNP K Ab is not considered to be a specific marker for the presence of the immune attack against hematologic stem cells. However, a case–control study on AA conducted by the International Agranulocytosis and AA Study revealed that a past history of RA is significantly associated with the subsequent development of AA [34], and previous studies revealed the presence of anti-

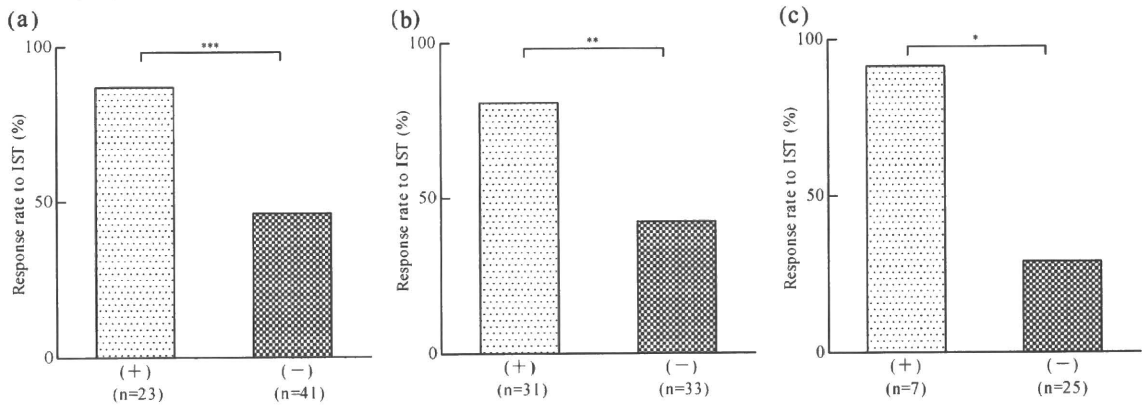

Fig. 4 The relationships between anti-hnRNP K Abs and response rate to IST in patients with BMF. The response rates to IST were compared between the following patient groups. **a** Patients with anti-hnRNP K Abs (+) and those without anti-hnRNP K Abs (−). **b** Patients showing at least one Ab^+ of three auto-Abs (+) and patients not showing Ab^+ in any of the three auto-Abs (−). **c** PNH^- patients with anti-hnRNP K Ab^+ (+) and those anti-hnRNP K Ab^- (−) (***P= 0.0015, **P=0.0022, *P=0.0265)

moesin Abs in 14% of patients with RA and in 37% of patients with AA [13, 35]. These findings suggest that AA and RA may share pathogenetic mechanisms characterized by a breakdown of immune tolerance to moesin and hnRNP K. It remains unclear why bone marrow failure develops only in AA despite the sharing of immune mechanisms. Although a breakdown of immune tolerance toward multiple autoantigens occurs in both diseases, the breakdown toward antigens on hematopoietic stem cells may occur only in patients with AA.

A strong correlation was found between the presence of anti-hnRNP K Abs and that of anti-DRS-1 Abs or anti-moesin Abs in patients with AA in the present study, indicating that a propensity of patients with immune-mediated AA thus undergo a breakdown of immune tolerance toward multiple autoantigens, possibly including pathogenic autoantigens in AA. Therefore, anti-hnRNP K Abs may serve as an indirect marker for the presence of immune pathophysiology of AA. Indeed, the presence of anti-hnRNP K Abs predicted a response to IST either by itself or in combination with anti-DRS-1 Abs or anti-moesin Abs, even in PNH^- patients with AA (Fig. 4). Among the three different Abs, only the presence of anti-hnRNP K Abs proved to be a significant factor for a good response to IST based on a multivariate analysis. Therefore, the detection of anti-hnRNP K Abs alone or together with anti-DRS-1 Abs and anti-moesin Abs may be useful in choosing the optimal therapy for AA patients, particularly when PNH-type cell detection is inapplicable. Recent reports showed that some patients with AA improved with anti-CD20 Ab (rituximab) therapy [36, 37]. The detection of these auto-Abs may also be useful for identifying AA patients who are likely to respond to such anti-CD20 Ab therapy.

Fritsch et al. [38] recently reported that hnRNP A2-specific T cell clones from patients with RA show a strong Th1 phenotype and secrete higher amounts of IFN-γ than Th1 clones from controls. Inhibition experiments performed with mAb specific to MHC class II molecules show that the hnRNP A2-induced T cell responses are largely HLA-DR restricted. $CD4^+$ T cells play an important role in the development of AA as well as of HLA-DRB1*1501 [9, 12]. Specific immune responses to hnRNP K may induce the polarization of Th1 $CD4^+$ cells and may thereby contribute to development of AA. Identification of hnRNP K-specific T cells with HLA class II tetramers and a functional analysis of those would help further clarify the roles of immune response specific to hnRNP K in the pathophysiology of AA.

Table 2 Pretreatment variables associated with a response to ATG plus CsA therapy

Favorable factors	*P* value	
	Univariate[a]	Multivariate[b]
Gender (male vs. female)	1.0000	0.8770
Age (at least 40 years vs. younger)	1.0000	0.4380
Severity (severe vs. moderate)	0.5085	0.8540
PNH-type cell (positive vs. negative)	0.0097	0.0370
Anti-DRS-1 Abs (positive vs. negative)	0.5610	0.7800
Anti-moesin Abs (positive vs. negative)	0.0036	0.5800
Anti-hnRNP K Abs (positive vs. negative)	0.0004	0.0120

[a] Fisher's exact probability test

[b] Wald c^2 test for a logistic regression model

Acknowledgments The authors would like to thank R. Oumi and T. Tanaka of Cellular Transplantation Biology of Kanazawa University who provided some technical assistance and all of the BMF study groups who provided sera of patients to this study. This work was supported by a grant from Grant-in-Aid for Scientific Research from the Ministry of Education, Science, Technology, Sports and Culture of Japan (KAKENHI No. 21390291) and grants from the Research Committee for Idiopathic Hematopoietic Disorders, the Ministry of Health, Labor, and Welfare, Japan.

References

1. Rosenfeld SJ, Kimball J, Vining D, Young NS (1995) Intensive immunosuppression with antithymocyte globulin and cyclosporine as treatment for severe acquired aplastic anemia. Blood 85 (11):3058–3065
2. Bacigalupo A, Broccia G, Corda G, Arcese W, Carotenuto M, Gallamini A, Locatelli F, Mori PG, Saracco P, Todeschini G, Coser P, Iacopino P, Vanlint MT, Gluckman E (1995) Antilymphocyte globulin, cyclosporin, and granulocyte colony-stimulating factor in patients with acquired severe aplastic anemia (SAA): a pilot study of the EBMT SAA Working Party. Blood 85(5):1348–1353
3. Maciejewski JP, Hibbs JR, Anderson S, Katevas P, Young NS (1994) Bone marrow and peripheral blood lymphocyte phenotype in patients with bone marrow failure. Exp Hematol 22(11):1102–1110
4. Nakao S, Yamaguchi M, Shiobara S, Yokoi T, Miyawaki T, Taniguchi T, Matsuda T (1992) Interferon-gamma gene expression in unstimulated bone marrow mononuclear cells predicts a good response to cyclosporine therapy in aplastic anemia. Blood 79 (10):2532–2535
5. Sloand E, Kim S, Maciejewski JP, Tisdale J, Follmann D, Young NS (2002) Intracellular interferon-gamma in circulating and marrow T cells detected by flow cytometry and the response to immunosuppressive therapy in patients with aplastic anemia. Blood 100(4):1185–1191
6. Takami A, Nakao S, Tatsumi Y, Wang HB, Zeng WH, Yamazaki H, Yasue S, Shiobara S, Matsuda T, Mizoguchi H (1999) High inducibility of heat shock protein 72 (hsp72) in peripheral blood mononuclear cells of aplastic anaemia patients: a reliable marker of immune-mediated aplastic anaemia responsive to cyclosporine therapy. Br J Haematol 106(2):377–384
7. Nakao S, Takamatsu H, Chuhjo T, Ueda M, Shiobara S, Matsuda T, Kaneshige T, Mizoguchi H (1994) Identification of a specific HLA class II haplotype strongly associated with susceptibility to cyclosporine-dependent aplastic anemia. Blood 84(12):4257–4261
8. Sugimori C, Chuhjo T, Feng XM, Yamazaki H, Takami A, Teramura M, Mizoguchi H, Omine M, Nakao S (2006) Minor population of CD55(-)CD59(-) blood cells predicts response to immunosuppressive therapy and prognosis in patients with aplastic anemia. Blood 107(4):1308–1314. doi:10.1182/blood-2005-06-2485
9. Sugimori C, Yamazaki H, Feng XM, Mochizuki K, Kondo Y, Takami A, Chuhjo T, Kimura A, Teramura M, Mizoguchi H, Omine M, Nakao S (2007) Roles of DRB1*1501 and DRB1*1502 in the pathogenesis of aplastic anemia. Exp Hematol 35(1):13–20. doi:10.1016/j.exphem.2006.09.002
10. Berger T, Rubner P, Schautzer F, Egg R, Ulmer H, Mayringer I, Dilitz E, Deisenhammer F, Reindl M (2003) Antimyelin antibodies as a predictor of clinically definite multiple sclerosis after a first demyelinating event. N Engl J Med 349(2):139–145
11. Ronkainen MS, Harkonen T, Perheentupa J, Knip M (2005) Characterization of the humoral immune response to glutamic acid decarboxylase in patients with autoimmune polyendocrinopathy-candidiasis-ectodermal dystrophy (APECED) and/or type 1 diabetes. Eur J Endocrinol 153(6):901–906. doi:10.1530/eje.1.02026
12. Feng XM, Chuhjo T, Sugimori C, Kotani T, Lu XZ, Takami A, Takamatsu H, Yamazaki H, Nakao S (2004) Diazepam-binding inhibitor-related protein 1: a candidate autoantigen in acquired aplastic anemia patients harboring a minor population of paroxysmal nocturnal hemoglobinuria-type cells. Blood 104(8):2425–2431. doi:10.1182/blood-2004-05-1839
13. Takamatsu H, Feng XM, Chuhjo T, Lu XZ, Sugimori C, Okawa K, Yamamoto M, Iseki S, Nakao S (2007) Specific antibodies to moesin, a membrane-cytoskeleton linker protein, are frequently detected in patients with acquired aplastic anemia. Blood 109 (6):2514–2520. doi:10.1182/blood-2006-07-036715
14. Nyman TA, Rosengren A, Syyrakki S, Pellinen TP, Rautajoki K, Lahesmaa R (2001) A proteome database of human primary T helper cells. Electrophoresis 22(20):4375–4382
15. Jensen ON, Podtelejnikov A, Mann M (1996) Delayed extraction improves specificity in database searches by matrix-assisted laser desorption/ionization peptide maps. Rapid Commun Mass Spectrom 10(11):1371–1378
16. Yates JR (1998) Mass spectrometry and the age of the proteome. J Mass Spectrom 33(1):1–19
17. Camitta BM (2000) What is the definition of cure for aplastic anemia? Acta Haematol 103(1):16–18
18. Caporali R, Bugatti S, Bruschi E, Cavagna L, Montecucco C (2005) Autoantibodies to heterogeneous nuclear ribonucleoproteins. Autoimmunity 38(1):25–32. doi:10.1080/08916930400022590
19. Hassfeld W, Steiner G, Hartmuth K, Kolarz G, Scherak O, Graninger W, Thumb N, Smolen JS (1989) Demonstration of a new antinuclear antibody (anti-RA33) that is highly specific for rheumatoid arthritis. Arthritis Rheum 32(12):1515–1520
20. GA DA, Vretou E, Sekeris CE (1988) Autoantibodies to the core proteins of hnRNPs. FEBS Lett 231(1):118–124
21. KE JL, Wilson SH, Steinberg AD, Klinman DM (1988) Antibodies from patients and mice with autoimmune diseases react with recombinant hnRNP core protein A1. J Autoimmun 1(1):73–83
22. Montecucco C, Caporali R, Negri C, de Gennaro F, Cerino A, Bestagno M, Cobianchi F, Astaldi-Ricotti GC (1990) Antibodies from patients with rheumatoid arthritis and systemic lupus erythematosus recognize different epitopes of a single heterogeneous nuclear RNP core protein. Possible role of cross-reacting antikeratin antibodies. Arthritis Rheum 33(2):180–186
23. Steiner G, Hartmuth K, Skriner K, Maurerfogy I, Sinski A, Thalmann E, Hassfeld W, Barta A, Smolen JS (1992) Purification and partial sequencing of the nuclear autoantigen RA33 shows that it is indistinguishable from the A2 protein of the heterogeneous nuclear ribonucleoprotein complex. J Clin Investig 90(3):1061–1066
24. Hassfeld W, Steiner G, Studnickabenke A, Skriner K, Graninger W, Fischer I, Smolen JS (1995) Autoimmune response to the spliceosome. An immunologic link between rheumatoid arthritis, mixed connective tissue disease, and systemic lupus erythematosus. Arthritis Rheum 38(6):777–785
25. Jones DA, Yawalkar N, Suh KY, Sadat S, Rich B, Kupper TS (2004) Identification of autoantigens in psoriatic plaques using expression cloning. J Investig Dermatol 123(1):93–100. doi:10.1111/j.0022-202X.2004.22709.x
26. Bomsztyk K, VanSeuningen I, Suzuki H, Denisenko O, Ostrowski J (1997) Diverse molecular interactions of the hnRNP K protein. FEBS Lett 403(2):113–115
27. Bomsztyk K, Denisenko O, Ostrowski J (2004) HnRNP K: One protein multiple processes. Bioessays 26(6):629–638. doi:10.1002/bies.20048
28. Mandal M, Vadlamudi R, Nguyen D, Wang RA, Costa L, Bagheri-Yarmand R, Mendelsohn J, Kumar R (2001) Growth factors regulate heterogeneous nuclear ribonucleoprotein K expression and function. J Biol Chem 276(13):9699–9704

29. Li C, Hong Y, Tan YX, Zhou H, Ai JH, Li SJ, Zhang L, Xia QC, Wu JR, Wang HY, Zeng R (2004) Accurate qualitative and quantitative proteomic analysis of clinical hepatocellular carcinoma using laser capture microdissection coupled with isotope-coded affinity tag and two-dimensional liquid chromatography mass spectrometry. Mol Cell Proteomics 3(4):399–409. doi:10.1074/mcp.M300133-MCP200
30. Hatakeyama H, Kondo T, Fujii K, Nakanishi Y, Kato H, Fukuda S, Hirohashi S (2006) Protein clusters associated with carcinogenesis, histological differentiation and nodal metastasis in esophageal cancer. Proteomics 6(23):6300–6316. doi:10.1002/pmic.200600488
31. Klimek-Tomczak K, Mikula M, Dzwonek A, Paziewska A, Karczmarski J, Hennig E, Bujnicki JM, Bragoszewski P, Denisenko O, Bomsztyk K, Ostrowski J (2006) Editing of hnRNP K protein mRNA in colorectal adenocarcinoma and surrounding mucosa. Br J Cancer 94(4):586–592. doi:10.1038/sj.bjc.6602938
32. Notari M, Neviani P, Santhanam R, Blaser BW, Chang JS, Galietta A, Willis AE, Roy DC, Caligiuri MA, Marcucci G, Perrotti D (2006) A MAPK/HNRPK pathway controls BCR/ABL oncogenic potential by regulating MYC mRNA translation. Blood 107(6):2507–2516. doi:10.1182/blood-2005.09.3732
33. Valai A, Belisova A, Hayer S, Hoefler E, Steiner G (2004) The RNA binding domains of hnRNP K contain major autoepitopes targeted by patients with SLE and other autoimmune diseases. In: ICI/FOCISed. Abstract number 1148
34. Kaufman DW, Kelly JP, Levy M, Shapiro S (eds) (1991) The drug etiology of agranulocytosis and aplastic anemia: the international agranulocytosis and aplastic anemia study. Oxford University Press, New York
35. Wagatsuma M, Kimura M, Suzuki R, Takeuchi F, Matsuta K, Watanabe H (1996) Ezrin, radixin and moesin are possible autoimmune antigens in rheumatoid arthritis. Mol Immunol 33 (15):1171–1176
36. Hansen PB, Lauritzen AMF (2005) Aplastic anemia successfully treated with rituximab. Am J Hematol 80(4):292–294. doi:10.1002/ajh.20428
37. Castiglioni MG, Scatena P, Pandolfo C, Mechelli S, Bianchi M (2006) Rituximab therapy of severe aplastic anemia induced by fludarabine and cyclophosphamide in a patient affected by B-cell chronic lymphocytic leukemia. Leuk Lymphoma 47(9):1985–1986. doi:10.1080/10428190600709630
38. Fritsch R, Eselbock D, Skriner K, Jahn-Schmid B, Scheinecker C, Bohle B, Tohidast-Akrad M, Hayer S, Neumuller J, Pinol-Roma S, Smolen JS, Steiner G (2002) Characterization of autoreactive T cells to the autoantigens heterogeneous nuclear ribonucleoprotein A2 (RA33) and filaggrin in patients with rheumatoid arthritis. J Immunol 169(2):1068–1076

Leukemia (2010) 24, 748–755

www.nature.com/leu

ORIGINAL ARTICLE

Lenalidomide induces cell death in an MDS-derived cell line with deletion of chromosome 5q by inhibition of cytokinesis

A Matsuoka[1], A Tochigi[1], M Kishimoto[1], T Nakahara[1], T Kondo[1], T Tsujioka[1], T Tasaka[1], Y Tohyama[2] and K Tohyama[1]

[1]Department of Laboratory Medicine, Kawasaki Medical School, Okayama, Japan; and [2]Division of Biochemistry, Faculty of Pharmaceutical Sciences, Himeji Dokkyo University, Hyogo, Japan

Myelodysplastic syndromes (MDS) are a group of hematopoietic stem cell disorders characterized by refractory cytopenias and susceptibility to leukemic transformation. On a subset of MDS patients with deletion of the long arm of chromosome5 (del(5q)), lenalidomide exerts hematological and cytogenetic effects, but the underlying pharmacological mechanisms are not fully understood. In this study, we have investigated the *in vitro* effects of lenalidomide on an MDS-derived cell line, MDS-L, which carries del(5q) and complex chromosome abnormalities. We found that the growth of MDS-L cells was specifically suppressed mainly by apoptosis, and in addition, multinucleated cells were frequently formed and finally died out in the presence of lenalidomide. Time-lapse microscopic observation and the DNA ploidy analysis revealed that lenalidomide does not affect DNA synthesis but inhibits cytokinesis of MDS-L cells. The gene expression profile showed decreased expression of M phase-related genes such as non-muscle myosin heavy-chain 10, polo-like kinase 1, aurora kinase B, citron kinase and kinesin family member *20A*(*KIF20A*). Interestingly, *KIF20A* is located at 5q31. These data contribute to the understanding of action mechanisms of lenalidomide on MDS with del(5q) and complex abnormalities.
Leukemia (2010) **24**, 748–755; doi:10.1038/leu.2009.296; published online 4 February 2010
Keywords: myelodysplastic syndrome; lenalidomide; cytokinesis; del(5q)

Introduction

The myelodysplastic syndromes (MDS) are a group of hematological disorders as a result of clonal growth of pathological stem cells and ineffective hematopoiesis.[1] Chromosomal abnormalities in marrow cells are found in 40–60% of MDS patients, and deletion of chromosome 5q (del(5q) /5q-) occupies 10–20% of the abnormalities.[2] Van den Berghe *et al.* reported a subtype of refractory macrocytic anemia characterized by isolated del(5q), normal or elevated platelet counts, abnormal hypolobated megakaryocytes and rare progression to acute myeloid leukemia.[3] This '5q- syndrome' is described as an independent clinical entity in the World Health Organization classification of MDS.[4]

Although the deleted area of 5q is different in case by case, del(5)(q32q33) is considered as a common deleted region.[5,6] The common deleted region expected in patients with 5q- syndrome is located distal to the region recognized in higher-risk groups with del(5q) that are susceptible to leukemic transformation.[6] Several hematopoiesis-related genes and tumor suppressor genes are located at 5q locus, and *SPARC*,[7] *CTNNA1*,[8] *EGR1*,[9] *RPS14*[10] and *CDC25C*[11] are reported as the candidate genes of MDS with del(5q) or 5q- syndrome.

Lenalidomide, a derivative of thalidomide, is shown to exert plenty of biological actions including inhibition of angiogenesis,[12] suppression of proinflammatory cytokine production such as TNF-α,[13] enhancement of T- and NK-cell activation.[14–16] Lenalidomide also brings about the improvement of erythropoiesis on MDS patients with del(5q) and in addition it is capable of eradicating the abnormal del(5q) clone.[17] Hence this drug has been paid attention as a specific therapeutic agent for MDS with del(5q). It is reported that lenalidomide inhibits the growth of CD34-positive cells having del(5q)[7] or Burkitt lymphoma cell lines[18] and that *SPARC* is upregulated by lenalidomide treatment,[7] but at present the target gene(s) of lenalidomide and its underlying action mechanisms are not determined yet.

In this study, we investigated the *in vitro* effects of lenalidomide on MDS-L, a myelodysplastic cell line with del(5q) and complex karyotypic abnormalities and searched the growth inhibition mechanism by lenalidomide.

Materials and methods

Reagents

Lenalidomide, generously provided by Celgene Corporation (Warren, NJ, USA) was dissolved in dimethylsulfoxide (DMSO) and stored at −20 °C. After thawing the stock solution it was protected from light and kept at 4 °C. According to the reported *in vitro* studies,[7,18,19] we used 10 μM lenalidomide and the final DMSO concentration was 0.01%.

Cell lines and culture

A human myeloblastic cell line, MDS-L[20] was derived as a subline from a myelodysplastic cell line, MDS92 which was established from the bone marrow of an MDS patient with del(5q).[21,22] MDS-L cells were positive for CD34, c-Kit, HLA-DR, CD13, CD33 and partially positive for CD41 and negative for CD3, CD14, CD20 and glycophorinA. The main karyotype was 49, XY, +1, der(5)t(5;19), −7, +8, −12, der(13)t(7;13), der(14)t(12;14), der(15)t(15;15), +19, +20, +21, der(22)t(11;22). Multicolor fluorescence *in situ* hybridization analysis indicated that MDS-L does not show a simple deletion of the single 5q locus but reveals a derivative small chromosome5 as a result of t(5;19)(q11;q13). Fluorescence in situ hybridization analysis targeting the 5q locus also indicated that the distal portion from 5q11.1 was certainly lost. MDS-L

Correspondence: Professor K Tohyama, Department of Laboratory Medicine, Kawasaki Medical School, 577 Matsushima, Kurashiki, Okayama 701–0192, Japan.
E-mail: ktohyama@med.kawasaki-m.ac.jp
Received 7 August 2009; revised 21 October 2009; accepted 9 November 2009; published online 4 February 2010

cells were maintained in RPMI1640 medium supplemented with 10% fetal bovine serum, 50 μM 2-mercaptoethanol, 2.0 mM L-glutamine and 100 U/ml IL-3. Lenalidomide (10 μM) or 0.01% DMSO were added daily during the experiments. Human myeloid leukemia cell lines carrying del(5q), HL-60 and KG-1 were also used. Cell growth was assessed by counting the number of living cells. The morphological assessment was performed with May–Gruenwald–Giemsa stained cytospin slides.

Apoptosis assay

The apoptosis was examined using AnnexinV Apoptosis Detection Kit (BD Pharmingen, San Diego, CA, USA) and all samples were analyzed by FACS Calibur flow cytometer and CellQuest software(Becton Dickinson, Franklin Lakes, NJ, USA).

Immunofluorescence study

MDS-L cells were centrifuged onto cytospin slides and fixed for 30 s in 4% formalin/50% acetone, then permeabilized with lysis buffer including 0.2% Triton X-100, 25 mM HEPES, 60 mM PIPES, 10 mM EGTA and 2 mM $MgCl_2$ for 30 s. Antibody staining was performed using mouse monoclonal anti-aurora kinase A (BD biosciences, San Jose, CA, USA), rabbit polyclonal anti-CDC25C(Santa Cruz Biotechnology, Santa Cruz, CA, USA) to detect centrosomes,[23] and AlexaFluor488- or AlexaFluor594-conjugated anti-IgG antibodies (Molecular Probes, Eugene, OR, USA) as secondary antibodies. The nucleus was stained with DAPI (Dojindo, Kumamoto, Japan). Cells were observed under an Olympus BX51 fluorescence microscope and a ×100/1.35 numerical aperture oil objective.

Live cell imaging by a time-lapse microscopy

Cells were seeded in 35 mm glass bottom culture dish and then 100 ng/ml Hoechst 33342 Dojindo was added for 1 h. Time-lapse imaging was performed on Zeiss Axiovert 200 M microscope (Zeiss, Göttingen, Germany) equipped with halogen light source, xenon lump, C4742-95ER digital camera and the Aquacosmos/ratio imaging system (Hamamatsu photonics K.K., Hamamatsu, Japan) at 37 °C and 5% CO_2. All images were collected using Zeiss Ph2 plan-NEOFLUAR ×40, 0.75 numerical aperture objective. Camera binning was 2 × 2, imaging times were 240 ms. Each image was captured every 2 min until the time points as indicated.

Cell-cycle and DNA ploidy analyses

Cells were fixed with 100% methanol for 60 min and treated with 2 mg/ml ribonuclease A (Nacalai Tesque, Kyoto, Japan) for 20 min at 37 °C, next with 50 μg/ml propidium iodide (PI; Sigma, St Louis, MO, USA) for further 20 min at room temperature. As to the analysis using bromodeoxyuridine (BrdU) and 7-amino-actinomycinD (7-AAD), the cells were pulse-labeled with 10 μM BrdU for 120 min and the cell-cycle assay was performed using BrdU Flow Kit (BD Pharmingen) and FACS Calibur flow cytometer. DNA ploidy was analyzed by the use of a laser-scanning cytometry as previously described.[24] Briefly, the cytospin samples stained with May–Gruenwald–Giemsa were captured with a CCD camera and their coordinates (*x* and *y*) on the slide were recorded. Next the identical smears were treated with 2 mg/ml ribonuclease A for 1 h at 37 °C and restained with 100 μg/ml PI, and the fluorescence intensity of each cell was quantified as the DNA contents together with the morphological assessment.

Statistical analyses

To compare the two nuclei of binucleated cells, we measured the surface area and DNA ploidy of each nucleus and calculated the Pearson product–moment correlation coefficients and the Sperman rank correlation coefficients.

Gene expression profiling

Gene expression profiling of MDS-L cells was examined in three independent experiments (lenalidomide-treated or DMSO-treated cells were harvested once on day 7 and twice on day 9). Total RNA was extracted with RNeasy Mini Kit (Qiagen, Germantown, MD, USA) and 5 μg of total RNA was amplified with the one-cycle cDNA synthesis and the one-cycle Target Labeling and Control Reagent packages (Affymetrix Santa Clara, CA, USA). Biotin-labeled fragmented cDNA was hybridized to Affymetrix-GeneChip Human Genome U133 Plus 2.0 Arrays covering >47,000 transcripts representing 39,000 human genes. Chips were washed and scanned with a GeneChip Scanner 3000 (Affymetrix).

Reverse transcription–polymerase chain reaction (RT–PCR)

Total RNA was extracted with RNeasy Mini Kit (Qiagen) and RT–PCR was performed using One step RNA PCR Kit (TAKARA BIO, Otsu, Japan) and following primers: *non-muscle myosin heavy-chain10(MYH10)* (sense:CATCTACAACCCTGCCACTC; antisense:TCCTCACGATCTTGAAGCATG), *aurora kinase B(AURKB)* (sense:ATGGCCCAGAAGGAGAACTC; antisense:TTCTCCCG AGCCAAGTACAC), *polo like kinase* (sense:ATGAGTGCTGCA GTGACTGC; antisense:GAGCAGCAGAGACYYAGGCA), *kinesin family member 20A* (*KIF20A*)(sense:CTAAATTACAGCAGTG CAAAGCAG; antisense:TTAGTACTTTTTGCCAAAAGGCCCAG), *CDC14A*(sense:CTCCATCGATGAGGAGCTGG; antisense:GAC AGGAGTGCTCTGTAGGC), *SPARC* (sense:CTGTGGCAGAGGT GACTGAG; antisense:GGCAGGAAGAGTCGAAGGTC), *glyceraldehydes-3-phosphate dehydrogenase (GAPDH)* (sense:GCC TCCTGCACCACCAACTG; antisense:CCCTCCGACGCCTGCTT CAC). PCR was performed using GeneAmp PCR system 9700 (Applied Biosystems, Tokyo, Japan) for 30 cycles, each consisting of 30 s at 94 °C, 30 s at 58 °C and 30 s at 72 °C.

Immunoblotting analysis

Cell lysates of MDS-L were prepared in lysis buffer containing 50 mM Tris-HCL, 150 mM NaCl, 5 mM EDTA, 0.5% TritonX-100, 0.05% sodium dodecyl sulfate (SDS), 0.5% sodium deoxycholate, 2 mM phenylmethylsulfonyl fluoride and 1 mM Na3VO4. Cell lysates were separated in SDS–polyacrylamide gel electrophoresis (SDS–PAGE) and immunoblotting analysis was performed as previously described.[25] Used primary antibodies were rabbit anti-KIF20A(Bethyl Laboratories, Montgomery, TX, USA) and mouse anti-aurora kinase B(BD Biosciences, San Jose, CA, USA).

Results

Treatment with lenalidomide inhibits the proliferation of MDS-L cell line

As lenalidomide is reported to inhibit the growth of CD34-positive cells with del(5q)[7] or Burkitt lymphoma cell lines,[18] we investigated the effect of lenalidomide on the growth of myeloid cell lines carrying del(5q). Daily addition of lenalidomide to *in vitro* culture did not show any suppressive effect on HL-60

(Figure 1a) nor KG-1 (data not shown). In contrast, MDS-L cells proliferated in the presence of IL-3 by day 4, but after that the cell number was gradually decreased together with appearance of dying or dead cells (Figures 1a and 2a). We analyzed apoptosis by dual staining of annexinV and PI, and found that lenalidomide induces apoptotic cell death onto a major part of MDS-L cells after around day 5 (Figure 1b).

MDS-L cells become multinucleated and polyploid by the treatment with lenalidomide

Lenalidomide-induced apoptosis to most of MDS-L cells, and we also found that lenalidomide treatment brought about the appearance of binucleated cells on day 4 (before the beginning of massive cell death) and subsequently multinucleated cells were often detected. On day 10 about a half of the cells which survived under lenalidomide treatment represented multinuclearity (Figures 2a and b).

In general, cell division consists of the two-step process: nuclear division (mitotic division) and subsequent cytoplasmic division (cytokinesis). Disturbance of either division might give rise to multinucleated cells. To examine whether the chromosome segregation ordinarily occurs or not, we compared the size and DNA contents of two nuclei of more than 100 binucleated cells by photomicrographic measurement and laser-scanning cytometry, respectively, and confirmed that the two nuclei were almost of the same size (the correlation coefficient between the two nuclei was 0.827) and such cells proved to be certainly 4N. These data indicate that lenalidomide treatment does not impair the DNA synthesis and that the chromosome segregation is normally accomplished to generate equally binucleated cells.

Next, we analyzed the cell-cycle pattern and the DNA ploidy of lenalidomide-treated MDS-L cells by flow cytometry. The percentage of subdiploid (<2N) cells was increased and instead diploid (2N) cells were decreased after lenalidomide treatment (Figure 3a). Furthermore, the cells with polyploidy such as tetraploid (4N) on day 4, and subsequently hyperpolyploid cells

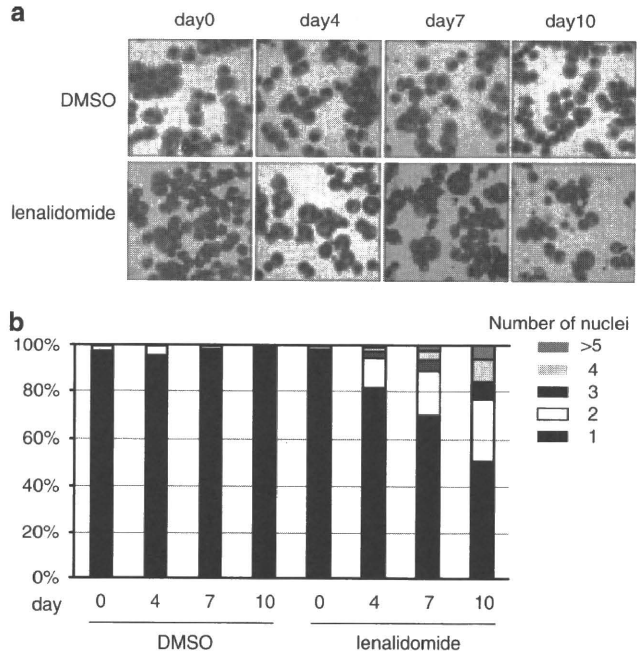

Figure 2 Lenalidomide induces the formation of multinuclearity in MDS-L cells. MDS-L cells were cultured in the presence of lenalidomide or DMSO as a control. (**a**) Morphological change of MDS-L cells during cultivation (May–Gruenwald–Giemsa stain). (**b**) The number of nuclei on each cell during cultivation (shown in percentage). Approximately 400 cells were counted on the indicated days.

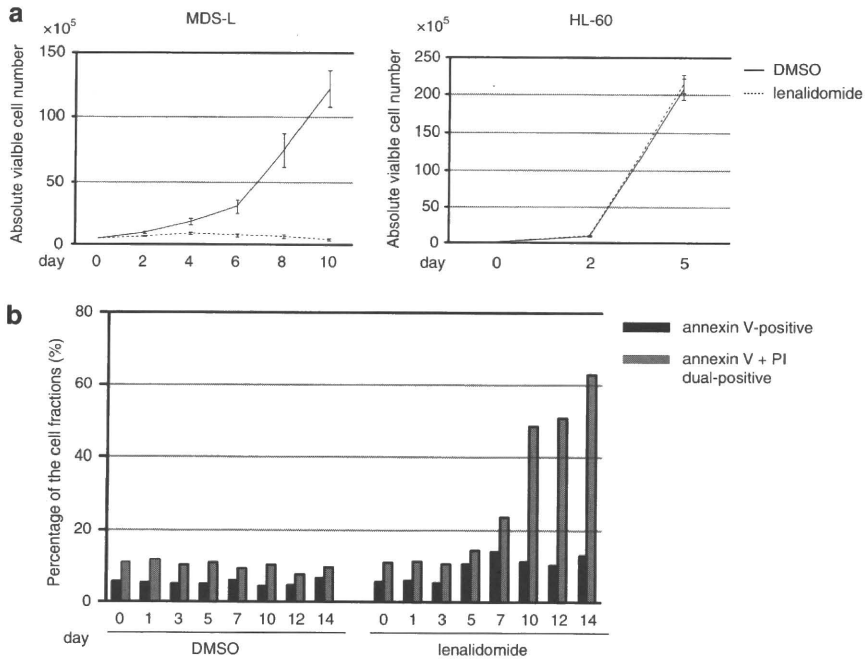

Figure 1 Lenalidomide inhibits the proliferation of MDS-L cells mainly by apoptosis. MDS-L and HL-60 cells were cultured in the presence of 10 μM lenalidomide or 0.01% DMSO as a control. (**a**) The cell number was counted on the indicated days. The data shown are the average ± s.d. of three independent experiments. (**b**) Apoptosis was assessed by flow cytometry using annexinV and propidium iodide (PI) staining on the indicated days. The percentages of only annexinV-positive cells (black column) and annexinV-PI dual-positive cells (gray column) are shown as the average of duplicate experiments.

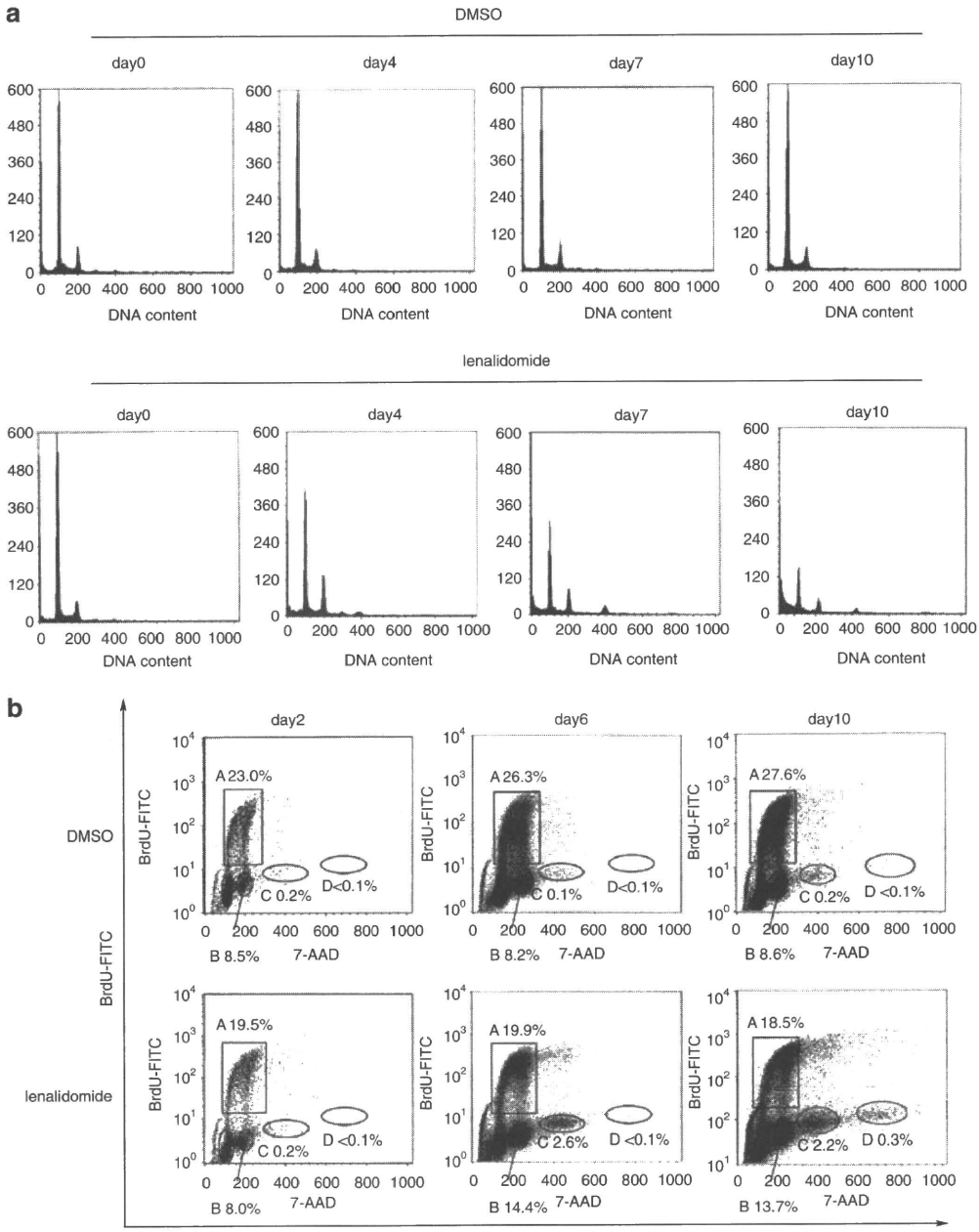

Figure 3 Lenalidomide induces the formation of polyploidy in MDS-L cells. (**a**) Cell-cycle analysis of MDS-L cells by propidium iodide (PI) staining. The cells treated with lenalidomide or DMSO for the indicated days were stained with PI for cell-cycle analysis. (**b**) Cell-cycle analysis of MDS-L cells by BrdU and 7-AAD dual staining assay. The cells treated with lenalidomide or DMSO for the indicated days were pulse-labeled for 120 min with bromodeoxyuridine (BrdU) and the incorporation of BrdU was measured together with quantification of DNA contents by 7-AAD by flow cytometry. Areas A and B indicate the fractions of ordinary diploid cells in S phase and G2/M phase, respectively. Areas C and D indicate the fractions of tetraploid and octoploid cells in G2/M phase, respectively. Ten-fold cells are plotted in the data of days 6 and 10 as compared with the data of day 2 to emphasize the presence of polyploid cells.

such as 8N and 16N were detected. Together with morphological finding, it was suggested that some parts of 4N cells entered the cell cycle again and formed hyperploid cells. The BrdU and 7-AAD dual-staining assay indicated that lenalidomide hardly inhibited DNA synthesis and a small part of the cells entered the next cell cycle from 4N to 8N to generate polyploid cells (Figure 3b). Taken together, a small part of the cells entered the next cell cycle to form multinucleated cells and finally they also died out.

Treatment with lenalidomide inhibits cytokinesis of MDS-L cells

As described above, lenalidomide treatment caused the increase in binucleated cells, but seemed not to affect DNA synthesis or mitotic division. Hence, we speculated that one of the direct action of lenalidomide is inhibition of cytokinesis. We observed lenalidomide-treated or control MDS-L cells by a time-lapse microscopy and chased the whole process of cell division. The control cells showed normal mitosis and cytokinesis and gave

rise to two daughter cells in more than 90% of observed cell division examples. In lenalidomide-treated cells, on the contrary, the cleavage furrow was formed after mitosis and the cells were about to divide into two daughter cells, but the cytokinesis was interrupted. The furrow became widened and finally binucleated cells were formed (Figure 4a). Such an aborted cytokinesis was ubiquitously detected by daily addition of lenalidomide, resulting in frequent appearance of multinucleated cells (Figure 4b, Figures 2a and b).

Treatment with lenalidomide suppresses the gene expression of M phase-related molecules in MDS-L cells

We harvested lenalidomide-treated or control MDS-L cells once on day 7 and twice on day 9, and investigated the gene expression profiling. The three independent studies represented almost the same pattern of gene expression profiles, and lenalidomide treatment resulted in the decreased gene expression of M phase-related molecules (Supplementary Table 1). Among them, the expression of *MYH10, aurora kinase B, PLK1, CDC14A* and *citron kinase* was particularly declined and these changes were also confirmed by RT–PCR (Figure 5a) and in part by immunoblotting analysis (data not shown).

As for the genes located at 5q, after lenalidomide treatment, the expression of *interferon regulatory factor 1 (IRF1)* and *KIF20A* was decreased to 0.43-fold (range: 0.34–0.49) and 0.41-fold (range: 0.05–0.65), respectively. Inversely, the expression of *early growth response 1 (EGR1), colony-stimulating factor 1*

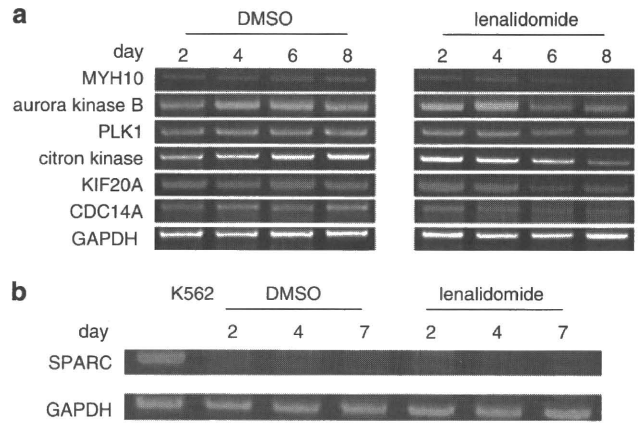

Figure 5 Lenalidomide treatment decreases the expression of M phase-related molecules. Changes in the expression of several M phase-related genes (*MYH10, aurora kinase B, PLK1, citron kinase, KIF20A, CDC14A*) (**a**) and *SPARC* (**b**) by semi quantitative RT–PCR in MDS-L cells cultured in the presence of lenalidomide or dimethylsulfoxide (DMSO) for the indicated days. K562 was used as a positive control and *GAPDH* as an internal standard.

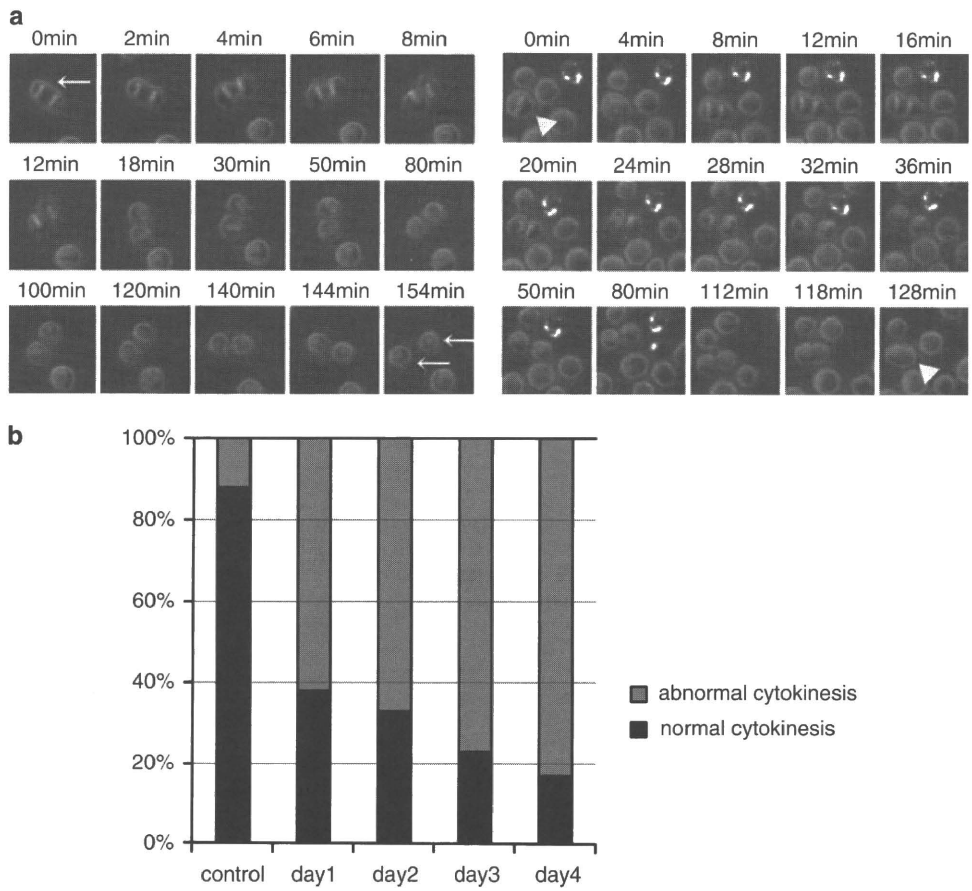

Figure 4 Lenalidomide inhibits cytokinesis of MDS-L cells. MDS-L cells were cultured for 4 days in the presence of lenalidomide or dimethylsulfoxide (DMSO) as a control, and on each day the aliquots of the cells were incubated with 100 ng/ml Hoechst 33342 for 1 h and the cell division was observed by a time-lapse microscopy. (**a**) Time-lapse images of the living cells during cell division. Arrows show a normal cell division. Arrowheads show a cell presenting abnormal cytokinesis. (**b**) The percentage of the cells presenting normal/abnormal cytokinesis was counted on the indicated days.

(*CSF-1R*) and *endothelial cell-specific molecule 2* (*ECSM2*) was increased to 11.5-fold (range: 4.7–26.5), 16.2-fold (range: 7.7–21.7) and 37.4-fold (range: 16.9–56.8), respectively. Expression of *SPARC* was rather weak or absent and not enhanced after lenalidomide treatment by RT–PCR (Figure 5b) and the gene expression profiling (data not shown).

Lenalidomide induces aberrant multiplication of centrosomes in MDS-L cells

We showed that lenalidomide induces cell death in part by formation of multinucleated cells by inhibition of cytokinesis. We also indicated that a part of polyploidy cells enter the next cell cycle (Figures 3a and b). Nigg[26] reported that the cells presenting aberrant centrosome number form multipolar spindle in the next M phase and are not able to survive because of a lack of essential genes. In fact, the mitotic cells with multiple centrosomes were observed frequently on day 4 after lenalidomide treatment in MDS-L cells (Figures 6a and b). These data suggested that aberrant multiplication of centrosomes caused by cytokinesis failure is one mechanism of lenalidomide-induced cell death.

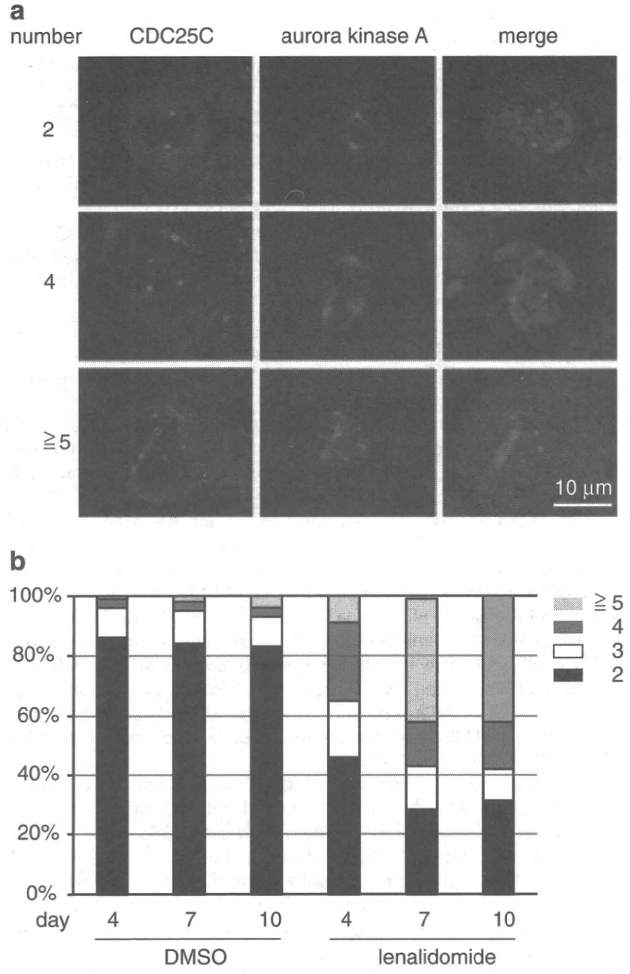

Figure 6 Lenalidomide induces aberrant multiplication of centrosomes in MDS-L cells. MDS-L cells treated with lenalidomide or dimethylsulfoxide (DMSO) were immunostained by anti-CDC25C and anti-aurora kinase A and corresponding AlexaFluor488- or AlexaFluor594-conjugated secondary antibodies. (**a**) Immunofluorescence staining of lenalidomide-treated MDS-L cells. The spots where CDC25C (green) and aurora kinase A (red) colocalized were considered as centrosomes. The chromosome area was stained with DAPI (blue) (magnification ×1000). (**b**) The number of the centrosomes in each cell (shown in percentage). More than hundred cells were examined for counting the number of centrosomes on the indicated days.

Discussion

There are important genes encoding or involved in tumor suppression, growth factors and their receptors, transcriptional factors at 5q locus, and certain genes might also be related to lenalidomide-specific growth suppression. In this study, we performed *in vitro* studies using MDS-L cell line which had been established from an MDS patient with del(5q) to further investigate del(5q)-related leukemogenesis and action mechanisms of lenalidomide.

MDS-L cell line carries a derivative small chromosome5 as a result of t(5;19)(q11;q13) and complex abnormalities instead of simple del(5q). Hence, this cell line should not be called as a typical 5q- cell line. However, an intensive study by Drexler *et al.*[22] confirmed that MDS92 (a parental cell line of MDS-L and carries the similar chromosome abnormalities including 5q change) shows the loss of BAC RP11-54C4 signal indicating 5q31-32 deletion. Therefore, MDS-L will be one of the available cell models with del(5q). Both HL-60 and KG-1 cell lines also represent del(5q) but neither of them showed growth suppression nor multinuclearity by lenalidomide treatment (data not shown). The effects of lenalidomide seem to be exerted exclusively on MDS-L cells.

Gandhi *et al.*[18] reported that lenalidomide shows an inhibitory effect on Namalwa cells by inducing G0/G1 arrest. Pellagatti *et al.*[7] reported that lenalidomide suppresses the growth of CD34-positive cells derived from the MDS with del(5q) and brings about the enhanced expression of *SPARC*. As for MDS-L, on the contrary, lenalidomide did not promote the expression of *SPARC* (Figure 5b). As one possible reason, the data by Pellagatti *et al.* seem to indicate mainly the effect on erythroid-lineage cells among the MDS progenitor cells but MDS-L cells are of the myeloid lineage and lacking in erythroid features. Another reason is that MDS-L cells carry various unknown genetic changes and might show different responses from the primary cells of 5q- syndrome to lenalidomide stimulation.

In this study, we showed that lenalidomide treatment induces multinuclearity by inhibition of cytokinesis in MDS-L cells (Figure 4). To date, several studies have indicated that the contractile ring which forms cell cleavage furrow involves various intracellular molecules: Rho-pathway molecules such as Rho GTPase, Rho kinase, citron kinase and formin; mitotic kinases, such as aurora kinase B and PLK1; molecules located on the central spindles, such as kinesin-like motors (MKLP1, MKLP2), ECT2 and MgcRacGAP.[26] Suppression of these molecules results in the formation of binucleated cells.[27,28] To approach the inhibitory mechanism of lenalidomide on cytokinesis of MDS-L cells, we inspected the gene expression profiles by microarray analysis and found decreased expression of M phase-related genes including cytokinesis-related molecules (Supplementary Table 1).

KIF20A (Rab6KIFL/MKLP2) is a kinesin-like protein, interacts with Rab6 that is associated with vesicular transport and has an important role in cytokinesis.[29,30] Interestingly, *KIF20A* is located at 5q31 and its expression was inhibited by lenalidomide treatment (Figure 5a). These results raise the possibility that *KIF20A* is one of the target genes of lenalidomide. It is also

reported that KIF20A associates with aurora kinase B and CDC14A phosphatase[31] and inhibition of *CDC14A* expression by siRNA method leads to the appearance of binucleated cells.[32] Myosin II is known to be involved in cytokinesis, and in our study the expression of *MYH10* was decreased by treatment of MDS-L with lenalidomide (Figure 5a), suggesting its relation to the inhibition of cytokinesis.

The cells which failed in cytokinesis bear multiple nuclei, and consequent multiplication of centrosomes causes impaired chromosomal segregation at the coming M phase and might result in mitotic cell death.[26,33] In fact, lenalidomide-treated MDS-L cells formed binucleated cells with four centrosomes around day 4 and then the cells with multiplicate centrosomes increased (Figure 6a). Such multinucleated cells with multiplicated centrosomes finally fall into cell death probably as a result of death induction by tetraploid checkpoint mechanism as reported by Andreassen.[34]

In our study, treatment of MDS-L cells with lenalidomide induces multinucleated cells, which are destined to die, and *KIF20A* located at 5q31 locus is proposed as a possible candidate target gene of lenalidomide. This investigation will contribute to molecular study of the myeloid malignancies with del(5q) and therapeutic mechanisms of lenalidomide. However, as MDS-L cells carry complex chromosome abnormalities besides the 5q change, the effects of lenalidomide on MDS-L might be attributable to some of the multiple genetic alterations.

The prognosis of MDS patients with del(5q) depends on various factors including additional chromosome abnormalities,[35–37] but lenalidomide exerts a favorable effect on 5q-MDS patients with complex abnormalities similarly as the patients with isolated del(5q) or to a lesser degree.[35,38,39] Our basic study might provide potentially useful issues to explain the clinical efficacy of lenalidomide on the patients with del(5q) and additional abnormalities.

Conflict of interest

K.T. has received research funding from Celgene K.K. The other authors declare no competing financial interests.

Acknowledgements

We thank Ms. Kazuko Yamane (Kawasaki Medical School) for her technical support.

This study was supported in part by the grant of the Japanese Cooperative Study Group for Intractable Bone Marrow Diseases, Ministry of Health, Labor and Welfare of Japan; in part by a Grant-in-Aid for Scientific Research from Japan Society for the Promotion of Science; and in part by Kawasaki Medical School Project Grant.

Authorship Contributions: K.T. designed the research and wrote the paper; A.M., A.T., T. N., T.K., and T.Ts. performed the experiments; M.K. performed statistical analyses; T.Ta. and Y.T. analyzed the results and contributed to useful discussion.

References

1 Heaney ML, Golde DW. Myelodysplasia. *N Engl J Med* 1999; **340**: 1649–1660.
2 Olney HJ, Le Beau MM. The cytogenetics of myelodysplastic syndromes. *Best Pract Res Clin Haematol* 2001; **14**: 479–495.
3 Van den Berghe H, Cassiman JJ, David G, Fryns JP, Michaux JL, Sokal G. Distinct haematological disorder with deletion of long arm of no. 5 chromosome. *Nature* 1974; **251**: 437–438.
4 Brunning RD, Orazi A, Germing U, Le Beau MM, Porwit A, Baumann I *et al.* Myelodysplastic syndromes. In: Swerdlow SH, *et al.* (eds). *WHO Classification of Tumours of Haematopoietic and Lymphoid Tissues*. IARC Press: Lyon, 2008, 87–107.
5 Boultwood J, Fidler C, Strickson AJ, Watkins F, Gama S, Kearney L *et al.* Narrowing and genomic annotation of the commonly deleted region of the 5q- syndrome. *Blood* 2002; **99**: 4638–4641.
6 Giagounidis AA, Germing U, Haase S, Hildebrandt B, Schlegelberger B, Schoch C *et al.* Clinical, morphological, cytogenetic, and prognostic features of patients with myelodysplastic syndromes and del(5q) including band q31. *Leukemia* 2004; **18**: 113–119.
7 Pellagatti A, Jädersten M, Forsblom AM, Cattan H, Christensson B, Emanuelsson EK *et al.* Lenalidomide inhibits the malignant clone and up-regulates the *SPARC* gene mapping to the commonly deleted region in 5q- syndrome patients. *Proc Natl Acad Sci USA* 2007; **104**: 11406–11411.
8 Liu TX, Becker MW, Jelinek J, Wu WS, Deng M, Mikhalkevich N *et al.* Chromosome 5q deletion and epigenetic suppression of the gene encoding alpha-catenin (CTNNA1) in myeloid cell transformation. *Nat Med* 2007; **13**: 78–83.
9 Joslin JM, Fernald AA, Tennant TR, Davis EM, Kogan SC, Anastasi J *et al.* Haploinsufficiency of EGR1, a candidate gene in the del(5q), leads to the development of myeloid disorders. *Blood* 2007; **110**: 719–726.
10 Ebert BL, Pretz J, Bosco J, Chang CY, Tamayo P, Galili N *et al.* Identification of RPS14 as a 5q- syndrome gene by RNA interference screen. *Nature* 2008; **451**: 335–339.
11 Wei S, Chen X, Rocha K, Epling-Burnette PK, Djeu JY, Liu Q *et al.* A critical role for phosphatase haplodeficiency in the selective suppression of deletion 5q MDS by lenalidomide. *Proc Natl Acad Sci USA* 2009; **106**: 12974–12979.
12 Dredge K, Marriott JB, Macdonald CD, Man HW, Chen R, Muller GW *et al.* Novel thalidomide analogues display anti-angiogenic activity independently of immunomodulatory effects. *Br J Cancer* 2002; **87**: 1166–1172.
13 Corral LG, Haslett PA, Muller GW, Chen R, Wong LM, Ocampo CJ *et al.* Differential cytokine modulation and T cell activation by two distinct classes of thalidomide analogues that are potent inhibitors of TNF-alpha. *J Immunol* 1999; **163**: 380–386.
14 Schafer PH, Gandhi AK, Loveland MA, Chen RS, Man HW *et al.* Schnetkamp PPEnhancement of cytokine production and AP-1 transcriptional activity in T cells by thalidomide-related immunomodulatory drugs. *J Pharmacol Exp Ther* 2003; **305**: 1222–1232.
15 Davies FE, Raje N, Hideshima T, Lentzsch S, Young G, Tai YT *et al.* Thalidomide and immunomodulatory derivatives augment natural killer cell cytotoxicity in multiple myeloma. *Blood* 2001; **98**: 210–216.
16 Muller GW, Chen R, Huang SY, Corral LG, Wong LM, Patterson RT *et al.* Amino-substituted thalidomide analogs: potent inhibitors of TNF-alpha production. *Bioorg Med Chem Lett* 1999; **9**: 1625–1630.
17 List A, Dewald G, Bennett J, Giagounidis A, Raza A, Feldman E *et al.* Lenalidomide in the myelodysplastic syndrome with chromosome 5q deletion. *N Engl J Med* 2006; **355**: 1456–1465.
18 Gandhi AK, Kang J, Naziruddin S, Parton A, Schafer PH, Stirling DI. Lenalidomide inhibits proliferation of Namalwa CSN.70 cells and interferes with Gab1 phosphorylation and adaptor protein complex assembly. *Leuk Res* 2006; **30**: 849–858.
19 Hideshima T, Chauhan D, Shima Y, Raje N, Davies FE, Tai YT *et al.* Thalidomide and its analogs overcome drug resistance of human multiple myeloma cells to conventional therapy. *Blood* 2000; **96**: 2943–2950.
20 Nakamura S, Ohnishi K, Yoshida H, Shinjo K, Takeshita A, Tohyama K *et al.* Retrovirus-mediated gene transfer of granulocyte colony-stimulating factor receptor (G-CSFR) cDNA into MDS cells and induction of their differentiation by G-CSF. *Cytokines Cell Mol Ther* 2000; **6**: 61–70.
21 Tohyama K, Tsutani H, Ueda T, Nakamura T, Yoshida Y. Establishment and characterization of a novel myeloid cell line from the bone marrow of a patient with the myelodysplastic syndrome. *Brit J Haematol* 1994; **87**: 235–242.